RESONANCE PROPERTIES OF OPEN PARALLEL-WIRE TRANSMISSION LINE SECTIONS AT 3000 MEGACYCLES/SECOND

by

DAVID C. COLL
Defence Scientific Service Officer
Defence Research Board

A THESIS

submitted in partial fulfillment of
the requirements for the degree of
Master of Engineering

McGill University
August, 1956

PREFACE

The research described in this paper was carried out in the Radio Research Laboratory, Department of Electrical Engineering, McGill University, under the direction of Dr. R.A. Chipman. The author would like to thank Dr. Chipman for his guidance, and the generosity with which he provided the extensive waveguide circuitry.

The author would also like to thank the Defence Research Telecommunications Establishment, Defence Research Board, for granting him Educational Leave with Financial Assistance so that he might spend this fruitful year at McGill. He is also indebted to DRTE for the loan of the 291A frequency meter.

The author was assisted during the measurements by Mr. Morris Pripstein, a final year Engineering Physics student. Mr. Pripstein's aid and interest were a great help.

Much of the precision machining for the project was done by Mr. V.Avarlaid and Mr. E.Ankups of the Eaton Electronics Laboratory, and the author wishes to express his appreciation of their cooperation.

Many thanks are due the author's sister-in-law, Barbara Maguire, for her excellent work in typing the MS.

DAVID C COLL

Montreal

August, 1956.

TABLE OF CONTENTS

ILLUSTRATIONS

INTRODUCTION

Resonant circuits are an important component of almost every radio circuit, and the determination of the properties of resonant circuits is an important measurement problem.

Circuits with distributed constants, such as transmission lines, may resonate if they are properly terminated. A resonant transmission line which is analogous to the familiar LRC series resonant circuit is called a reaction, or absorbtion, type resonator. One which is analogous to a parallel resonant circuit is called a transmission type resonator. The approach to the subject is governed by the type of resonator under consideration.

At the high frequencies at which radiation from open transmission lines becomes excessive, sections of completely closed waveguide are used as resonant circuits. The Q factor, or selectivity, of these cavities is usually very high. The Q values of some typical cavities are listed below.

These Q values have been calculated for a resonant frequency of 3000 Mc/s. The conducting surfaces of the cavities are assumed to be pure silver. Expressions for the Q's are found in Montgomery[1](pp 295 to 307).

TABLE I

Type of Cavity	Dimensions	Mode	Q
Coaxial	Radius of outer conductor = 5 cm. Ratio of radii = 3.6	TEM	9720
Rectangular	3" x 1½"	TE_{102}	17020
Cylindrical	Diam.= 10 cm.	TE_{112} TM_{012} TE_{012}	21500 26100 36600

Open parallel wire resonators would have their applications as resonant circuits, at microwave frequencies, if their Q's were high enough. They are simply constructed and completely ventilated. The extension of radio frequency techniques to the microwave regions has resulted in the design of tubes which are ideally suited to the use of parallel wire tuning circuits. Their ventilated property suits them to use in any device which measures changes in some property of the atmosphere, which affects the Q value. For example, a device such as the atmosphere refractometer.

The purpose of the research described in this paper was the investigation of resonance properties of open parallel wire sections at 3000 Mc/s. Previous work at McGill had demonstrated that the radiation from such lines could be considerably reduced by terminating the sections in transverse

metallic discs, a few wavelengths in diameter. If the terminations are considered as reflectors for the fields surrounding the wires, it seems reasonable that discs would intercept and reflect more of the energy than simple shorting bars.

The effect of the diameter of the conductors, and their separation, upon the Q factors of the resonant sections has been studied.

The order in which the paper is presented is given below:

A summary of the research performed at McGill on the radiation resistance of parallel wire lines, which is the precedent for the present work, is given in Chapter 1.

Chapter 2 deals with the theoretical aspects of the problem. Any calculation of the Q's is complicated by the determination of the energy storage and the termination losses. These quantities contain a complicated integral. However, this problem has been solved and is included in Appendix I as a contribution to the theory of parallel wire lines.

A summary of the microwave techniques used for the measurements of Q values is given in Chapter 3.

Chapter 4 is an analysis of a loop coupled (parallel resonant) circuit which forms the theoretical basis of the experimental method which was used. This method was originated by E. D. Reed of the Bell Laboratories. His analysis has been extended to include probe coupled (series resonant)

circuits. This extension is contained in Appendix II.

A description of the experimental procedure, and a discussion of the advantages, disadvantages, and errors of the method used are presented in Chapter 5.

Chapter 6 contains a description of the apparatus.

The results of the research and conclusions about it are given in Chapter 7. Some suggestions for further research are also given.

1. Radiation Resistance Studies at McGill.

The research described in this paper is based on studies of the effect of radiation upon the resonance properties of parallel wire transmission lines. This work was carried out in the Electrical Engineering Department under the direction of Dr. Chipman between 1950 and 1951 by Hoy, Carr, Boucher and Yurko.[2] Their research clarified the doubt existing about the value of the radiation resistance of parallel wire transmission lines, both short-circuited and open-circuited.

1.1 Value of Radiation Resistance.

The fact that imperfect terminations led to radiation of power from the line, was realized as long ago as 1900. However, the value of the resistance which would account for the radiation losses was a point of controversy for the next fifty years. The results of the work by Hoy, et al, indicate that there is no radiation from the length of the line; and that the radiation resistance of a line shorted at each end, by bars of the same diameter as the conductors, is given by:

$$R_{rad} = 120 \left(\frac{\pi s}{\lambda}\right)^2$$

This was predicted by King for lines shorted at each end and an even number of half-wavelengths long. This

value was also found by Mannebach, Pistolkors, Sterba and Feldman, and Whitmer for lines open circuited at both ends. An excellent historical account of the theoretical and experimental work done on the radiation from parallel wire lines may be found in Yurko's thesis.

1.2 Reduced Radiation Resistance.

Means for reducing the radiation resistance and increasing the Q's of resonant sections of such lines were proposed by Yurko. He suggested bringing the ends of a long line together to form a tapered line. He found that this reduced the losses due to radiation. Working at 1100 Mc/s he found that terminating the line with a transverse, circular, conducting disc (1.4 λ in diameter), rather than the shorting bars, greatly increased the Q of a shorted section.

In 1954, C. D. Pearse[3], working between 600 and 1600 Mc/s, investigated the effect of the diameter of the terminations on the radiation from various line lengths. He concluded that the optimum diameter was not critical and lay between 2.5λ and 3.5λ. Pearse found that the radiation resistance was reduced to 2 or 3% of the value for lines terminated in shorting bars or open circuits, and reported Q values of 2000 to 3500. He also found that the radiation resistance depended to a small degree on the length of the line.

1.3 Chipman Method.

The method used in all of these experiments was the Chipman method,[4] which requires a plot of the response of the resonator as a function of frequency. This was found by coupling the exciting power to the resonator through a small loop, so placed that only the transmission line mode would be excited. The energy in the resonator was detected by means of another small loop, which was connected to the heater of a thermocouple. In Hoy and Carr's work the output of the thermocouple was amplified in a chopper amplifier and used to drive an Esterline-Angue moving chart recorder. Yurko describes the errors in their work as: the non-linearity of the amplifier, the non-rectaliniarity of the chart, the disregarding of the finite size of the conductors, the use of improper shorting bars, the variable coupling losses, and the possible excitation of the antenna, or symmetric, mode. Yurko used the thermocouple output to drive the pen of a Leeds and Northrup Speedomax recording μvoltmeter.

The procedure in Hoy's, Carr's and Yurko's work was to vary the length of the resonating section in synchronism with the chart speed, to calibrate the horizontal chart axis in frequency and in this way obtain a plot of the response curve. Boucher investigated parallel rings, and used a mechanically tuned oscillator and fixed lengths.

The Chipman method is very convenient since it yields the Q curve directly, and is easily applied to Q and radiation resistance measurements on parallel wire lines. However, these disadvantages are apparant:

1) The Q measured is the loaded Q, and as such is dependent on the enviroment in which the resonator finds itself. That is, it is depen dent on the losses coupled into the resonator. The universal unloaded Q may be calculated from a series of results if the external losses are considered constant as seen by the resonator. However, varying the length of the resonator changes the degree of coupling, and hence the loaded Q. The subsequent error would be most noticeable for low Q resonators.

2) The use of the resonator during the experiments as a double-ended device entails the insertion of two coupling loops into the fields of the resonator. This increases the coupled losses and, hence, reduces the Q which is being measured.

3) The possibility of exciting some very low Q mode in the resonator, which would displace the zero level of the response curve, would lead to a large error. This change in base level was checked during the above experiments and found to be negligible.

4) There does not exist any way of determining the losses of the coupling system absolutely. The effect of the coupling loop insertion was indicated by the changes in the observed Q. The losses were assumed to be constant and small during the measurements because it required a large insertion of the coupling loop into the resonator before any noticeable change occurred in the resonant frequency or half-power bandwidth of the response curve. The coupling was maintained loose so that the resonator was not greatly disturbed by external losses, nor by the presence of the loop itself.

5) Because of the necessity for loose coupling, it was experimentally impossible to critically couple the resonator to the transmission line. Critical coupling is the coupling at which the resonator is matched to the line, i.e., the VSWR on the input line is 1 at critical coupling. This is therefore the most efficient position of operation.

6) The experimental resonators consisted of a large horizontal ground plane, which served as one termination, and the experimental terminations on the other end of the vertical transmission line. The procedure required the variation of

the length of the line and contact was maintained at the ground plane by means of nickel-plated brass spring-fingers. Also, the terminating discs used by Pearse were approximately three feet in diameter and were supported from the center at the top. These conditions lead to indeterminant contacts at the bottom and the possibility of non parallelism of the top and bottom terminations. It has been seen in the work at the higher frequency that such items are very important. However, at the lower frequencies at which he worked, the gradients of the fields involved are not so severe compared with the physical dimensions of the apparatus, thus minor mechanical aberrations are not so important. Also, the contact losses were most likely small compared to the radiation and coupling losses so that they would not contribute significantly to the final results. These possible losses have been ignored by the previous researchers since, in their method, the losses merely loaded the resonator and were indistinguishable from coupled losses.

2. Theoretical Considerations and the Calculation of a Q.

2.1 The definition of Q.

2.1.1 The Q factor may be defined on an energy basis as

$$Q = 2\pi \frac{\text{total energy stored in the electric and magnetic fields of the resonant system}}{\text{energy dissipated per cycle}} \qquad 2.1$$

It may also be expressed in terms of the average power lost in the resistances loading the resonator as

$$Q = \omega_0 \frac{\text{total energy stored in the electric and magnetic fields of the resonant system}}{\text{average power loss}} \qquad 2.2$$

2.1.2. For a resonant circuit coupled to a transmission line it is possible to define three values of Q. They are:

The unloaded Q

$$Q_U = \omega_0 \frac{\text{total energy .....}}{\text{average power loss in the resonant circuit alone}} \qquad 2.3$$

The external Q

$$Q_E = \omega_0 \frac{\text{total energy .....}}{\text{average power loss in the characteristic resistance of the transmission line as seen by the resonator}} \qquad 2.4$$

The loaded Q

$$Q_L = \omega_0 \frac{\text{total energy .....}}{\text{total average power loss}} \qquad 2.5$$

The three Q's are related by the equation:

$$\frac{1}{Q_L} = \frac{1}{Q_U} + \frac{1}{Q_E} \qquad 2.6$$

2.1.3 From transmission line theory, we obtain a definition of Q in terms of the line parameters. If we call this Q_T, then

$$Q_T = \frac{\beta}{2\alpha} \qquad 2.7$$

where:

β = the phase constant in radians/metre.

α = the attenuation constant in nepers/metre.

Since,

$$\beta = \frac{2\pi}{\lambda}$$

Q_T may also be expressed as

$$Q_T = \frac{\pi}{\lambda\alpha} \quad , \qquad 2.8$$

where

λ = the wavelength on the line.

It will be convenient to list the values of α for unshielded and shielded parallel cylinder lines. Assuming that skin effect is fully developed:

$$a_u = \frac{\frac{R_s}{\pi d} \frac{(s/d)}{[(s/d)^2 - 1]^{1/2}}}{120 \cosh^{-1} (s/d)} \qquad 2.9$$

$$a_s = \frac{\frac{R_s}{\pi d}\left[1 + \frac{1+2p^2}{4p^4}(1-4q^2)\right] + \frac{4R_s}{\pi D} q^2\left[1 + q^2 - \frac{1+4p^2}{8p^4}\right]}{120\left\{\ln\left(2p\frac{(1-q^2)}{(1+q^2)}\right) - \frac{1+4p^2}{16p^4}(1-4q^2)\right\}} \qquad 2.10$$

These expressions allow for proximity effect. The symbols used are defined in Figure 2.1

2.2 Quantities required for Calculation.

In order to calculate the Q value of a resonant section it is evident from the above definitions that the total energy stored and the power lost in the boundaries of the system are required. The unloaded Q will be calculated for it is the only one which is universal, i.e., independent of all external circuits and coupling systems.

In the process of resonance, the energy oscillates between the electric and magnetic fields. When the magnetic field is at its maximum value, the total energy is stored in it. Hence we may calculate the total energy

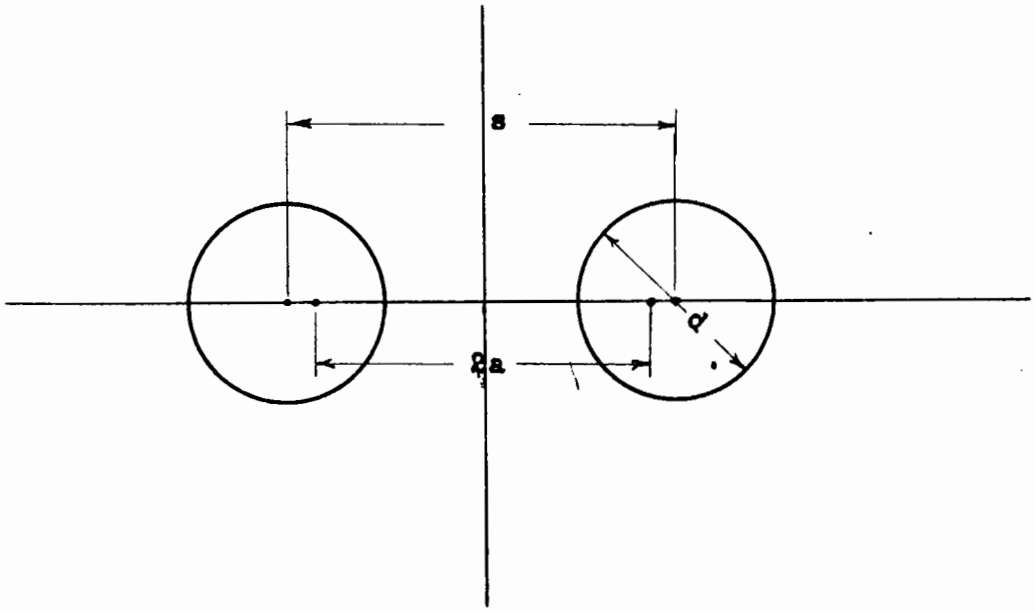

Open line.

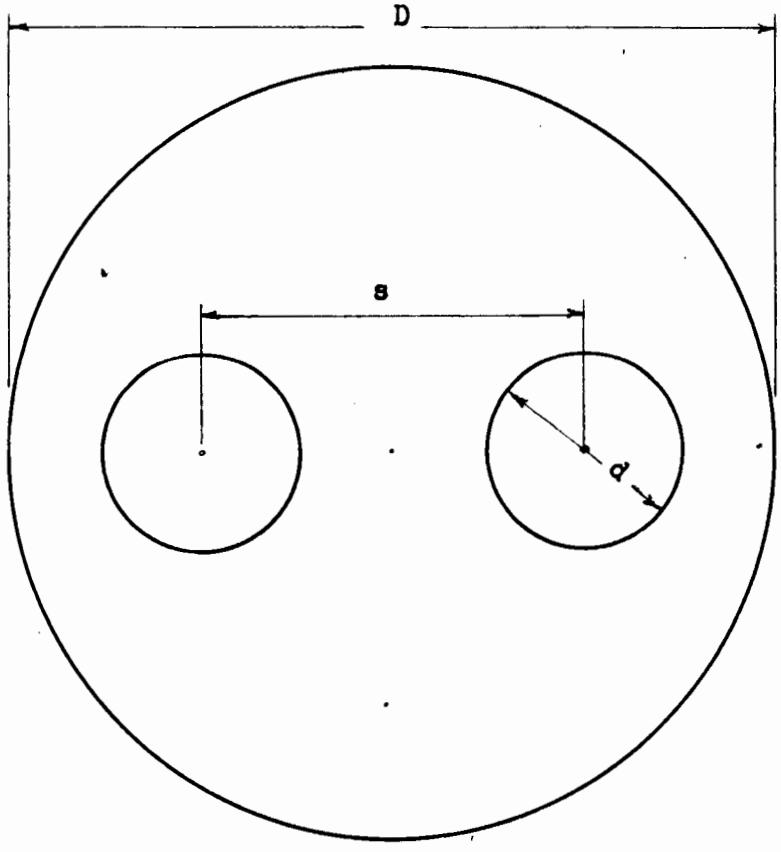

$p = \frac{s}{d}$

$q = \frac{s}{D}$

Shielded line

Figure 2.1 Dimensions of open and shielded parallel wire transmission lines.

stored by evaluating the familiar integral

$$\tfrac{1}{2}\,\mu \int_V H^2 \, dv$$

when the magnetic field is at a maximum value with respect to time.

To calculate the losses in the boundaries, a knowledge of the currents flowing in them is required. It is permissible to assume that skin effect is fully developed. Therefore, the only currents flowing will be surface currents and numerically equal to the tangential magnetic fields at the boundaries.

2.3 Fields of an infinitely long parallel cylinder line.

Consider the electromagnetic field distribution surrounding two, infinitely long, parallel, circular cylinders.

Assume that equal and opposite currents, I, flow in the cylinders. The cylinders may then be replaced by line currents, of value I, separated by a distance 2a, where:

$$a^2 = (s/2)^2 - (d/2)^2 \qquad 2.11$$

and

s = the separation of the center lines of the conductors

d = the diameter of the cylinders.

In rectangular coordinates (Figure 2.2) the electric and magnetic fields of symmetrically placed cylinders are:

$$E_x = \frac{V_o}{\cosh^{-1}(s/d)} \left[\frac{x-a}{\sqrt{(x+a)^2 + y^2}} - \frac{x+a}{\sqrt{(x-a)^2 + y^2}} \right]$$

$$E_y = \frac{V_o}{\cosh^{-1}(s/d)} \left[\frac{y}{\sqrt{(x-a)^2 + y^2}} - \frac{y}{\sqrt{(x+a)^2 + y^2}} \right]$$

$$H_x = \frac{I}{2\pi} \left[\frac{y}{\sqrt{(x+a)^2 + y^2}} - \frac{y}{\sqrt{(x-a)^2 + y^2}} \right]$$

$$H_y = \frac{I}{2\pi} \left[\frac{x-a}{\sqrt{(x-a)^2 + y^2}} - \frac{x+a}{\sqrt{(x+a)^2 + y^2}} \right]$$

The magnetic field lines are a family of circles with centers on the line joining the centers of the conductors. The electric field lines are a set of circles, orthogonal to the first, with centers on the right bisector of the line joining centers of the conductors.

The field components are those of the transverse electromagnetic wave (TEM) which is represented by the static distribution propagating along the line. We shall call this mode of propagation the transmission line mode. Had we considered the symmetric case in which the current flowed the same way on both conductors, we would have arrived at the field components for the so-called antenna mode.

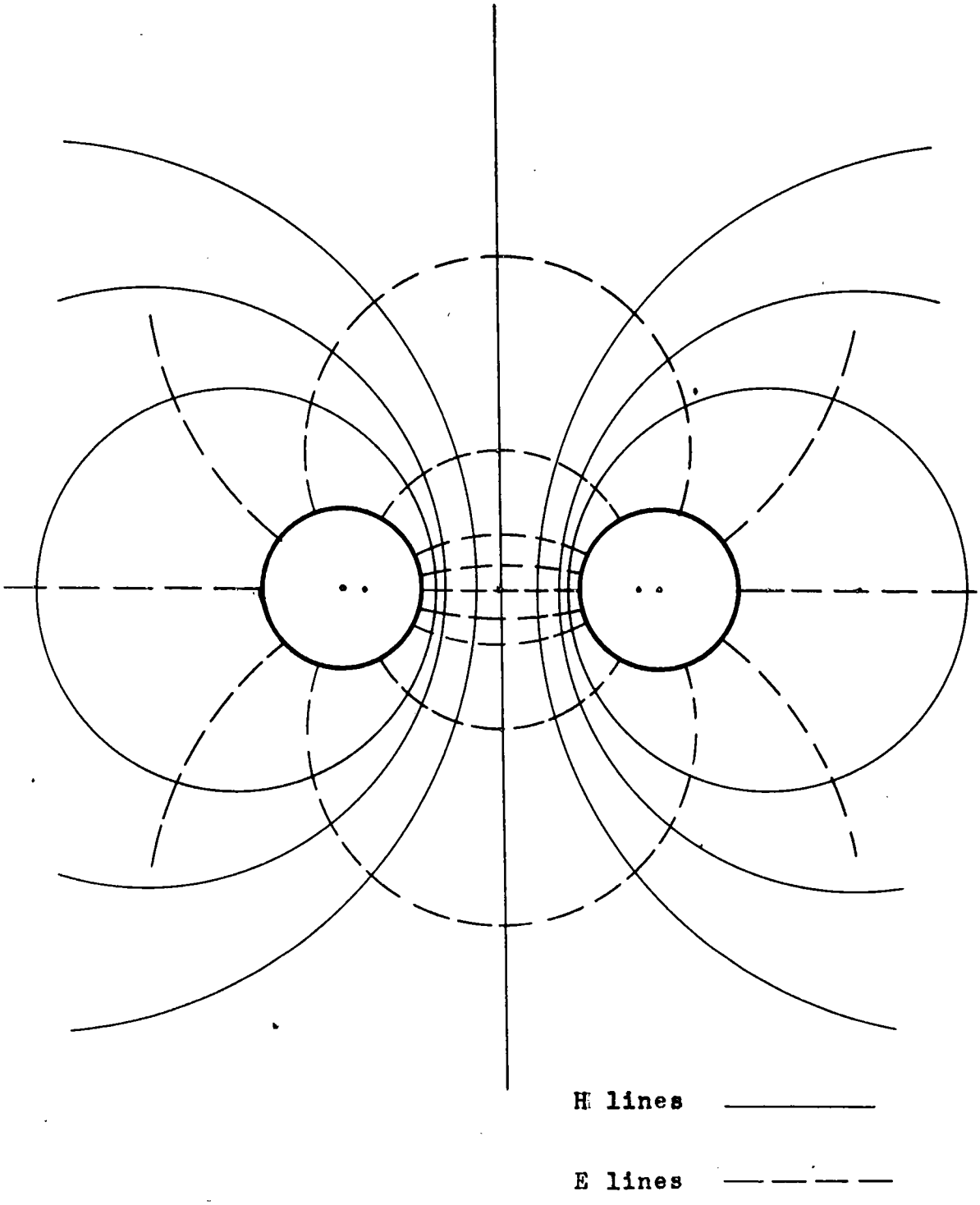

Figure 2.2 Electromagnetic fields of two parallel circular cylinders.

The total magnetic field squared is given by:

$$H^2 = H_x^2 + H_y^2$$

$$= \left(\frac{I}{2\pi}\right)^2 \frac{4a^2}{\left[(x+a)^2 + y^2\right]\left[(x-a)^2 + y^2\right]}$$

2.4 Energy storage and losses in an unshielded resonant section.

The energy consists of a sinusoidal wave which is propagating along the line. When short circuits are placed at current nulls, a standing wave is produced. Since the losses at each reflection from the shorts are small, the amplitude of the standing wave grows with each reflection. But, since it is the sum of many sine waves, it is still a sine wave. At each point on the line where a null in the standing wave occurs, the fields are distorted by the finite current which flows in the line to overcome its resistance. Thus, the standing wave is an approximation to a sine wave, and may be further distorted by small phase shifts at the reflections.

2.4.1 A cosinusoidal distribution of current with distance along the line is assumed. The total energy stored in the resonator is then

$$E = \tfrac{1}{2}\cdot\tfrac{1}{2}\,\mu\ell \int_A H^2\, da \qquad 2.14$$

where:

E = the total energy stored in the resonator in joules.

μ = permeability of air.

A = area of an infinite transverse plane exclusive of the area covered by the conductors.

ℓ = the length of the resonant section in metres.

H = peak magnetic field on the line.

The length of the section may be calculated accurately from the resonant frequency.

$$\ell = \frac{n\lambda}{2} = \frac{1}{2}\,\frac{nc}{f_o} \qquad 2.15$$

where:

n = the number of half-cycle variations of current along the length of the section.

c = the velocity of propagation of the energy = the velocity of light in air.

f_o = the resonant frequency.

2.4.2 The average conductor losses, including both conductors, are

$$L_c = \tfrac{1}{2}\cdot\tfrac{1}{2}I^2R_c\cdot\ell \qquad 2.16$$

where:

L_c = the average power lost in the conductors in watts.

I = the peak value of the current (= maximum value at the terminations with respect to time).

R_c = the conductor resistance, which including proximity effect is:

$$R_c = \frac{2R_s}{\pi d} \quad \frac{(s/d)}{\left[(s/d)^2 - 1\right]^{1/2}} \qquad 2.17$$

R_s = the surface resistivity of the conductors.

2.4.3 The average termination losses, including both terminations are

$$L_t = 2R_s \int_{A'} \tfrac{1}{2}H^2 da \qquad 2.18$$

where:

L_t = the average power loss in the terminations in watts.

R_s = the surface resistivity of the terminations in ohms/square.

A' = the area of the terminations exclusive of the area covered by the conductors.

2.4.4 The radiation losses may be assumed to have a form similar to that found by previous experimenters. That is, we shall assume, a radiation resistance of the form

$$R_{rad} = k'' \pi^2 (s/\lambda)^2 \qquad 2.19$$

Storer and King predicted a value of k" of 120 for lines with both open and short circuit terminations. This value includes the effect of the terminations as rad-

iating elements. Since an infinitely long line would have a radiation resistance of zero, radiation from a finite line is inseparable from the effects of the terminations. The value of k" will be greatly reduced by terminating the line in large transverse discs. It is possible that for conductors large compared to the wavelength the form of R_{rad} will require further modification due to the shielding effect of the conductors.

2.4.5 Summary.

Let us make the following definitions.

Let $$\int_A H^2 da = k \left(\frac{I}{2\pi}\right)^2 \qquad 2.20$$

$$\int_{A'} H^2 da = k' \left(\frac{I}{2\pi}\right)^2 \qquad 2.21$$

$$\frac{(s/d)}{[(s/d)^2 - 1]^{1/2}} = K \qquad 2.22$$

also, $$R_{rad} = (1/2\pi)^2 R \qquad 2.23$$

i.e. $$R = k''(2\pi^2 s/\lambda)^2$$

The energy stored and losses may be expressed in terms of these quantities as:

$$E = (I/2\pi)^2 \tfrac{1}{4} \mu l k$$

$$L_c = (I/2\pi)^2 \frac{2\pi R_s K \ell}{d}$$

$$L_t = (I/2\pi)^2 R_s k'$$

$$L_r = (I/2\pi)^2 R \qquad 2.24$$

2.5 Q_c, the calculated Q.

From the definition of Q in terms of power the calculated Q, Q_c, is

$$Q_c = \frac{2\pi^2 f \ell k \times 10^{-7}}{R_s \left[k' + \frac{2\pi K \ell}{d} \right] + R} \qquad 2.25$$

The values of k and k' have been found in terms of s, d, and the termination radius ρ, as shown in Appendix I. The evaluation of the definite integral envolves the use of a known conformal mapping. The solution of this integral greatly simplifies the labour envolved for anyone who is interested in parallel-wire lines with circular terminations.

2.6 Shielded sections.

Shielding the resonant section by a cylindrical tube which makes close contact with the terminations, transforms the open line to a shielded-pair line. This shielding contains the fields within the section and eliminates the radiation losses.

The object in investigating the shielded line would be to obtain results for a line in which the radiation resistance was zero. The conductor losses may be calculated from the expression of section 2.1.3; however, the termination losses are indeterminant since the field distribution is not known. These losses are independent of length and hence can be calculated from a series of results, taken for the same conductor diameters and spacing.

The addition of the shield forces the field distribution to change so that the boundary conditions will be satisfied. To what degree the fields are disturbed in the vicinity of the conductors and within the half-power circle, where the fields have their greatest values, is a matter of conjecture. From the values obtained for k' (Appendix I), it is reasonable to assume that the fields near the outer periphery of the terminations are insignificant; and hence that the field lines are distorted in a region where they are very small. As the diameter of the shield increases, this modification of the field pattern decreases. So, for a reasonably large shield, the values of the energy stored and the termination losses, which in this case contain the same integral, should be approximately the same as those for an open line. The complexity of the fields render any exact calculation of the losses and energy storage a formidable problem, even numerically.

It is possible that the currents which flow in the shield, and hence across the termination-shield contact, cause more losses than the radiation resistance in the unshielded case. These currents would also increase the termination losses. Thus while the shielded Q is larger than the unshielded Q, it might not be as great as expected. The previous experimenters at McGill compared the shielded and unshielded values of Q in order to obtain the radiation resistance of the lines. Since the shields used were comparable to a wavelength in diameter, the effect of the shield on the fields should have been considered, because the shield does more than just eliminate the radiation.

3. Microwave Q measuring techniques.

In the initial search for a method which was readily adaptable to the problem at hand, two lines of approach were possible.

The first was to extend the response curve method used in the radiation resistance measurements; or to use some other technique which could be extended to 3000 Mc/s.

The second was to apply some microwave measurement technique to the problem. It was decided to follow the latter path because of the experience to be gained.

The conventional approach towards the determination of the response of a resonant circuit, and hence its Q factor, is to obtain the input impedance of the circuit as a function of frequency. This may be done by measuring the impedance directly, or by measuring the VSWR or reflection coefficient (which are functions of impedance).

A summary of some of the microwave techniques which have been used to measure Q factors will demonstrate the convenience and usefulness of the reflected power method that has been used.

Measurements on resonant circuits fall into two classes: point by point determination of the characteristic under investigation as a function of frequency; and panoramic displays of the characteristic. The relative merits of the two general methods are noted during the summary.

Some of the methods outlined are applicable to transmission type resonators and others to reaction resonators. For application of any of these methods it is advised that the reference be consulted.

3.1 Method A

This method, which is contained in King's book,[5] utilizes the variation of the VSWR on the input line in the vicinity of resonance.

For application to this method the input impedance of the resonant circuit, as seen from the line, is expressed as

$$Z_{in} = \frac{1}{n^2}\left\{R' + jR'Q_o\left(\frac{2\Delta f}{f_o}\right)\right\}$$

The coupling losses have been neglected. The quantities are as shown in the transformer equivalent circuit.

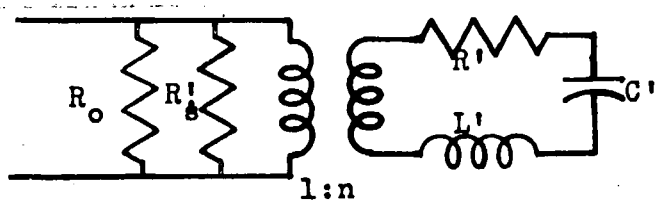

Figure 3.1 Equivalent circuit of a probe coupled resonator.

The half power points of the response curve are the points at which the resistive part of the impedance is equal to the reactive part. The frequency difference from resonance of these points are designated as $\pm \Delta f$, and the Q's are defined as the ratio of the appropriate $2\Delta f$ to the resonant frequency.

On the circle transmission line chart (Smith chart), the locus of the impedance of a resonant circuit is a circle. If the coupling losses are neglected this locus passes through the infinity point of the chart. If the resonator is overcoupled the impedance locus contains the center (1,0) point of the chart. If it is undercoupled it does not contain this point.

The VSWR's corresponding to resonance ($\Delta f=0$), $f \pm \Delta f_U$, $f \pm \Delta f_E$ and $f \pm \Delta f_L$ are the intersections of the impedance locus with the lines $x=0$, $x=r$, $x=1$ and $x=r+1$, respectively. x and r are the normalized components of the impedance. These intersections are the frequencies at which the reactive part of the input impedance is equal to the resistance appropriate to the definitions of Q_U, Q_E, and Q_L.

After f_o and the VSWR at resonance (S_o) have been found, graphs are used to find S_L, the VSWR at Δf_L. Thus, tuning the frequency until the VSWR is S_L yields Δf_L and Q_L may be calculated from the expression,

$$Q_L = \frac{f_o}{2\Delta f_L}$$

and Q_E and Q_U from,

$$S_o = \frac{Q_E}{Q_U} \quad \text{under coupled}$$

$$S_o = \frac{Q_U}{Q_E} \quad \text{over coupled}$$

and,

$$\frac{1}{Q_L} = \frac{1}{Q_U} + \frac{1}{Q_E}$$

If the coupling losses are significant, the impedance locus does not pass through the infinity point and the above method does not hold. However, a technique for handling such cases is described in the reference.

3.2 Method B

This second method is suggested by Hamilton,[6] et al, for the cold testing of oscillator cavities. It requires a plot of the VSWR, as a function of frequency, in the vicinity of resonance; and a knowledge of the VSWR at resonance S_o, and off resonance, S_1. It is also necessary to know the degree of coupling.

The reflection coefficient of the circuit is expressed as,

$$r = \left\{ \frac{(S_1-1)^2(S_o-S_1)^2\delta^2 + (S_o-1)^2}{(S_1+1)^2(S_o-S_1)^2\delta^2 + (S_o+1)^2} \right\}^{\frac{1}{2}}$$

where:

$$\delta = 2Q_E \frac{\Delta f}{f_o} \quad \text{overcoupled } (S_o > 1)$$

$$\delta = \frac{1-S_o S_1}{S_o - S_1} \delta \quad \text{undercoupled } (S_o < 1)$$

By use of the relation

$$S' = \frac{1+r}{1-r}$$

it is possible to plot S' versus S_o with S_1 as a parameter, if δ is assigned a definite value (such as 1). Knowing S_o and S_1 from the experimental data, a value of S' may be found at which Δf may be measured, corresponding to $\delta = 1$. Then Q_E and Q_o may be calculated from the relations,

$$\frac{\Delta f}{f_o} = \frac{1}{Q_E} \qquad \text{overcoupled}$$

$$\frac{\Delta f}{f_o} = \frac{1-S_o S_1}{Q_U} \qquad \text{undercoupled}$$

and

$$\frac{Q_U}{Q_E} = S_o - S_1$$

S_1 is always considered to be less than 1.

This method includes the finite coupling losses by allowing the VSWR off resonance, S_1, to be less than infinite.

3.3 Method C.

This method is known as the decrement method and is described by King.[5] It is suitable for the measurement of very high Q's only. (of the order of 10^4).

It is based on the fundamental definition of Q, as expressed by the decay constant of an excited resonator,

$$\frac{V_2}{V_1} = e^{-\frac{\omega_o}{2Q}(t_2-t_1)}$$

where; V_2 and V_1 are the amplitudes of the voltage across the circuit at times t_2 and t_1, respectively. The amplitude ratio and time delay may be measured by an oscilloscope with a fast triggered sweep and a variable delay.

3.4 Comparison.

Methods A and B are point to point methods and method C is a single frequency method. Methods A and B are best suited to the measurement of relatively low Q's.

The disadvantages of a method which involves the measurement of standing wave ratios are these:

In a microwave system VSWR is usually measured by means of a probe inserted into the transmission line through a slot. The probe is placed at a position of maximum field on the line and the SWR meter adjusted to

its index; the probe is then moved to a position of minimum field and the SWR read. The meter usually requires a modulated signal.

In order to obtain a smooth curve of VSWR versus frequency, it is necessary to take readings very close together, especially for high Q circuits. This places a strict condition on the frequency stability of the signal source and its modulation characteristic. If many resonators are to be tested the number of individual measurements becomes prohibitive.

Also, unless an attenuation substitution method is used to measure the SWR the methods depend on the square law characteristics of the detectors.

The panoramic, or sweep frequency methods, are more suited to the determination of resonator characteristics because an oscillographic display of the response, as a function of frequency, may be obtained by sweeping the oscilloscope with the source modulation. The sweep frequency methods have the advantage of not depending on the frequency stability of the apparatus, and eliminating the many single frequency measurements needed to produce the same curve.

These methods depend on the type of resonator which is being studied. In the study of transmission resonators the response of the test piece is usually compared

to the response of some reference circuit. The reference circuit may act as a frequency marker, in which case the power through the test piece must be known so that the half power points can be determined. Or, the response curves may be made coincident and the unknown Q found by comparison to a calibrated reference circuit. In the study of reaction type resonators the reflection coefficient of the device is measured by comparing the incident and reflected powers as a function of frequency.

3.5 Method D.

This is the Sproull and Linder[7] method for comparing the response curves of two transmission type resonant circuits. The apparatus shown in Figure 3.2 may be operated in several ways. One is to subtract the responses in the mixer circuit. Then, if the reference amplitude is one-half of the test amplitude, when the reference dip touches the zero level the wavemeter is oscillating at a half power point. It is also possible to calibrate the display by using the reference dip as a frequency marker.

The conditions on the apparatus are these:

1. The coupling must be very loose so that the Q will not be seriously affected by external losses. This is necessitated by the fact that the loaded Q is measured.

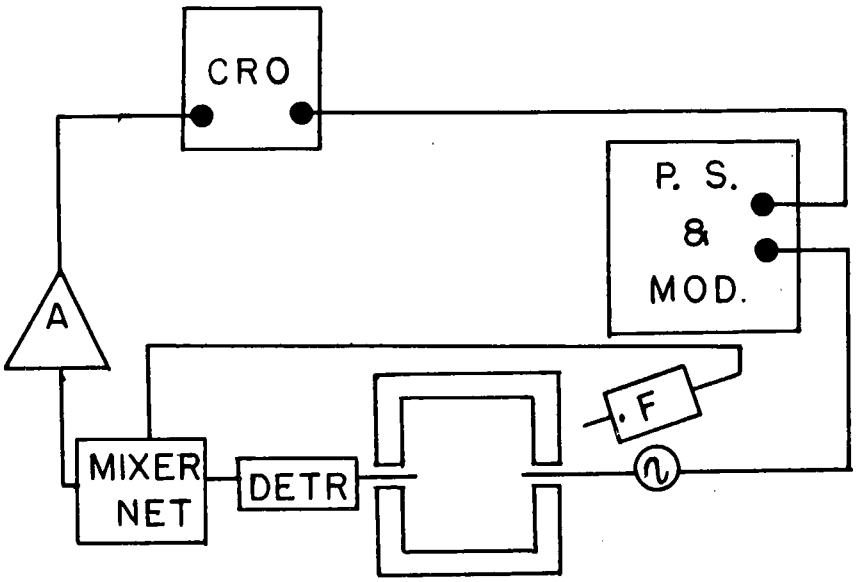

Figure 3.2 Apparatus - Sproull & Linder.

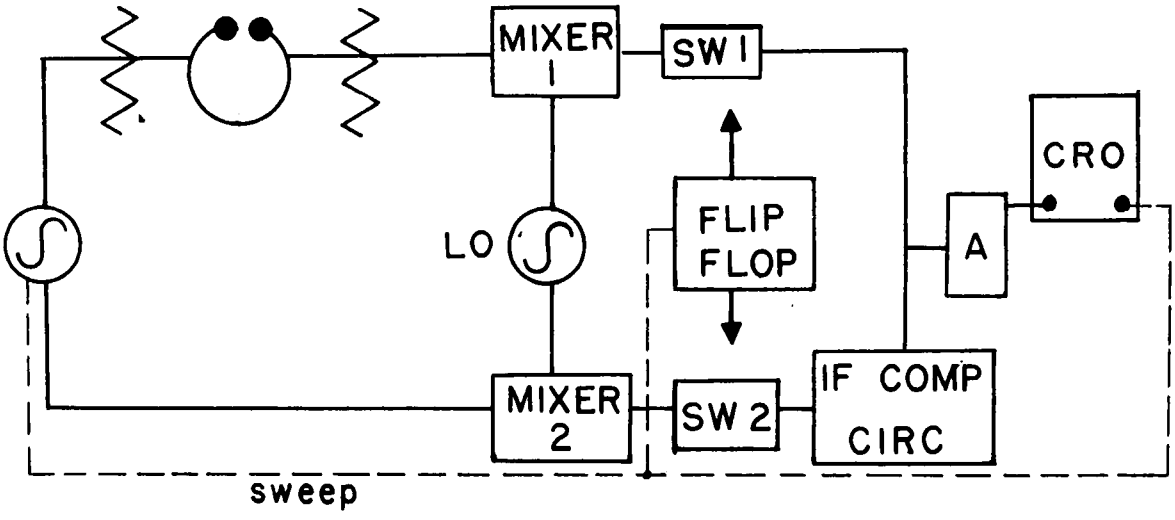

Figure 3.3 Apparatus - LeCaine.

2. The crystal detector must be a square law device.

3. The bandwidth of the coupling system must be greater than that of the test piece.

4. The amplifier must be linear, if the display is to be calibrated.

5. There must be no amplitude modulation of the source, since the response curve would be formed partially by this amplitude modulation.

6. The frequency modulation of the source must be linear.

3.6 Method E.

Lecaine[8] of the NRC has modified the Sproull and Linder method. He has introduced a superhetrodyne circuit in which the response of the test piece is compared to the response of an IF resonant circuit whose Q is known and variable, as in Figure 3.3. The responses are displayed on alternate sweeps of a CRO.

When the response curves are made coincident by varying the IF circuit, the frequency differences at the half power points are identical and the unknown Q may be calculated from the expression:

$$\frac{Q_{RF}}{Q_{IF}} = \frac{f_{RF}}{f_{IF}}$$

This method was applied to the measurement of Q's between 5000 and 15,000, with an error estimated to be ±3%.

The advantages of the Lecaine method over that of Sproull and Linder are these:

1. This method eliminates reading the half-power frequency difference from the face of the CRT.
2. The superhetrodyne detection system is very sensitive, hence the coupling can be very weak.
3. The response law of the crystals used as mixers is more reliable than that of the crystals used as detectors.
4. All components other than the mixers are common to both channels, hence reducing the need for linearity in the circuit.

3.7 Method F.

Montgomery[1] describes elaborate apparatus which has been developed at the M.I.T. Radiation Laboratory for the measurement of cavity Q's.

One is a system employing an FM discriminator with tunable IF amplifiers which places pips at the half power points of a response curve. The half power level is not too accurately found by this method.

He also describes apparatus called a cavity Q comparator which operates on the Sproull and Linder idea.

The above methods all yield the loaded Q value and require very light coupling in order to obtain an approximation to the true Q. There is nothing in the procedures except for the reduction in the Q which indicates the actual degree of coupling or the coupling losses.

4. Theory of Measurements.

The method which was used in the experiments will now be described.[9] It is first necessary to know the form of the reflection coefficient of a resonant circuit as a function of frequency.

4.1 The equivalent circuit of a resonant section and the variation of input impedance and reflection coefficient with frequency.

A resonant section of transmission line which is magnetically (loop or iris) coupled to a transmission line may be represented by an equivalent circuit, the coupling system being represented by an ideal transformer with external losses.

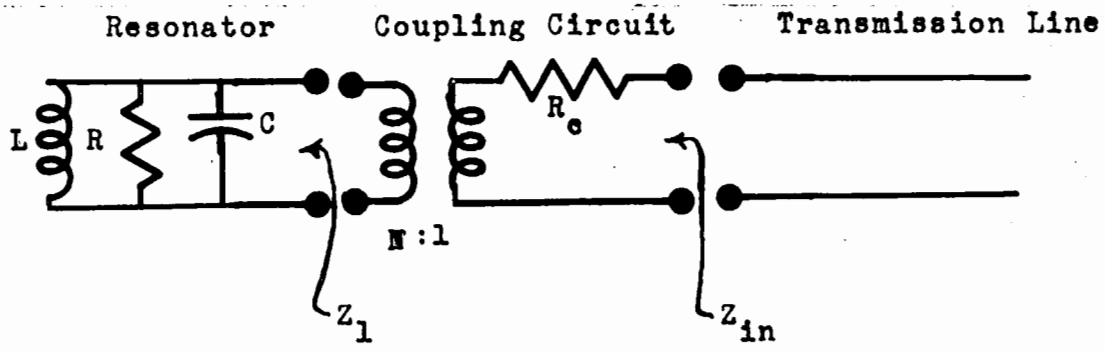

Figure 4.1 The equivalent circuit of a single ended resonator.

The input impedance of the cavity alone Z_1 may be written

as

$$Z_1 = \frac{1}{\frac{1}{R} + j(\omega C - \frac{1}{\omega L})} \tag{4.1}$$

if we define

$$\omega_o^2 = \frac{1}{LC} \tag{4.2}$$

$$\Delta\omega = \omega_o - \omega \tag{4.3}$$

and

$$M = \left(\frac{C}{L}\right)^{\frac{1}{2}} \tag{4.4}$$

then, in the vicinity of resonance,

$$Z_1 = \frac{1}{\frac{1}{R} + jM\frac{2\Delta\omega}{\omega_o}} \tag{4.5}$$

and the input impedance as seen from the transmission line is

$$Z_{in} = R_c + \frac{1}{N^2(+\frac{1}{R} + j2M\frac{\Delta\omega}{\omega_o})} \tag{4.6}$$

where R_c = the coupling system resistance.

Normalizing the input impedance with respect to the characteristic impedance R_o of the transmission line we obtain,

$$\frac{Z_{in}}{R_o} = \frac{R_c}{R_o} + \frac{1}{(\frac{R_o N^2}{R} + j2MR_oN^2\frac{\Delta\omega}{\omega_o})} \tag{4.7}$$

now, off resonance the resonator impedance becomes very small and we may express Z_{in} as

$$\frac{Z_{in}}{R_o} = \frac{R_c}{R_o} \qquad 4.8$$

similarly, at resonance where $\Delta\omega = 0$,

$$\frac{Z_{in}}{R_o} = \frac{R_c}{R_o} + \frac{R}{R_o N^2} \qquad 4.9$$

Recalling the familiar definition of the reflection coefficient, r,

$$r = \frac{\frac{Z_{in}}{R_o} - 1}{\frac{Z_{in}}{R_o} + 1} \qquad 4.10$$

the reflection coefficient off resonance, r_1, is

$$r_1 = \frac{\frac{R_{in}}{R_o} + 1}{\frac{R_c}{R_o} + 1} \qquad 4.11$$

since the coupling resistance R_c is much less than the characteristic impedance R_o; r_1 will usually be approximately equal to -1.

The reflection coefficient at resonance r_o is,

$$r_o = \frac{\left(\frac{R_c}{R_o} + \frac{R}{R_o N^2}\right) - 1}{\left(\frac{R_c}{R_o} + \frac{R}{R_o N^2}\right) + 1} \qquad 4.12$$

from these expressions we obtain

$$\frac{R}{R_o} = \frac{1 + r_1}{1 - r_1} \qquad 4.13$$

$$\left(\frac{R}{R_o} + \frac{R}{R_o N^2}\right) = \frac{1 + r_o}{1 - r_o} \qquad 4.14$$

and

$$\frac{R}{R_o N^2} = \frac{2(r_o - r_1)}{(1 - r_o)(1 - r_1)} \qquad 4.15$$

and hence can write the normalized input impedance as

$$\frac{Z_{in}}{R_o} = \frac{1 + r_1}{1 - r_1} + \frac{1}{\frac{(1 - r_o)(1 - r_1)}{2(r_o - r_1)} + j2MR_o N^2 \frac{\Delta\omega}{\omega_o}} \qquad 4.16$$

The value of the unloaded Q_o may be expressed in terms of our defined quantities as,

$$Q_o = \omega_o CR = MR \qquad 4.17$$

Similarly, the external Q_E is

$$Q_E = MR_o N^2 \qquad 4.18$$

where $R_o N^2$ is the external loading as seen by the resonator.

The degree of coupling may be expressed in terms of Q_o and Q_E as follows:

if $Q_o = Q_E$ the resonator is critically coupled and $r_o = 0$.

if $Q_o < Q_E$ the resonator is under coupled and r_o is negative.

if $Q_o > Q_E$ the resonator is overcoupled and r_o is positive.

we may rewrite equation 4.15 as

$$\frac{Q_o}{Q_E} = \frac{2(r_o - r_1)}{(1 - r_o)(1 - r_1)} \qquad 4.19$$

we may also rewrite equation 4.16 for the normalized input impedance as,

$$\frac{Z_{in}}{R_o} = \frac{1 + r_1}{1 - r_1} + \frac{2(r_o - r_1)}{(1-r_o)(1-r_1) + j\delta 2(r_o - r_1)} \qquad 4.20$$

where

$$\delta = Q_E \frac{2\Delta\omega}{\omega_o} = Q_E \frac{2\Delta f}{f_o} \qquad 4.21$$

We now express the reflection coefficient as a function of frequency in terms of r_o, r_1, and δ.

$$r = \frac{\frac{1+r_1}{1-r_1} + \frac{2(r_o - r_1)}{(1-r_o)(1-r_1) + j\delta 2(r_o-r_1)} - 1}{\frac{1+r_1}{1-r_1} + \frac{2(r_o - r_1)}{(1-r_o)(1-r_1) + j\delta 2(r_o-r_1)} + 1} \qquad 4.22$$

However, the quantity we are interested in, and are able to measure, is the square of the reflection coefficient, which is the ratio of reflected power to incident power.

$$|r|^2 = \frac{4r_1^2 (r_o-r_1)^2\delta^2 + r_o^2 (1-r_1)^4}{4(r_o-r_1)^2 \delta^2 + (1-r_1)^4} \qquad 4.23$$

This expression forms the basis of the measurement of Q by reflected power.

It is interesting to notice the similarity between the expression just derived and the one derived in the "Cold test" method discussed in reference 6. The latter is in terms of VSWR, but reduces to equation 4.23 when VSWR is expressed in terms of the reflection coefficient. The VSWR method is a point to point method and requires a different approach to the final result for over and

under coupled cases. Whereas the reflected power method only requires reading a different portion of a graph for the two cases, as will be seen.

4.2 Theory of procedure.

If a display of reflected power versus frequency can be experimentally obtained, the values of $|r_o|^2$, $|r_1|^2$ and f_o may be read from it directly. If the degree of coupling is known, the sign of r_o is determined. Then a family of curves may be plotted from equation 4.23 with Q_E as the parameter and the one which coincides with the experimental display yields the correct value of Q_E. This would be an accurate method of determining Q_E, but very lengthy. It is more practical to plot equation 4.23 for a fixed value of δ and with r_1 as the parameter, as in Figure 4.2. Then, having obtained the values of $|r_o|^2$, $|r_1|^2$, and f_o from the display a value, $|r^1|^2$, of $|r|^2$ at which δ = a known value may be found from the graph and $\Delta\omega$ measured at this power level. Q_E may then be found from equation 4.21, where $2\Delta\omega$ is the total bandwidth of the reflected power curve at the specified power level. Q_o may be calculated from equation 4.19.

The value of δ which was most convenient for determination of $2\Delta\omega$, was determined by the degree of coupling. For highly over coupled cases $\delta = \frac{1}{2}$ was a proper value; for under coupled cases $\delta = 2$ was a good value. The

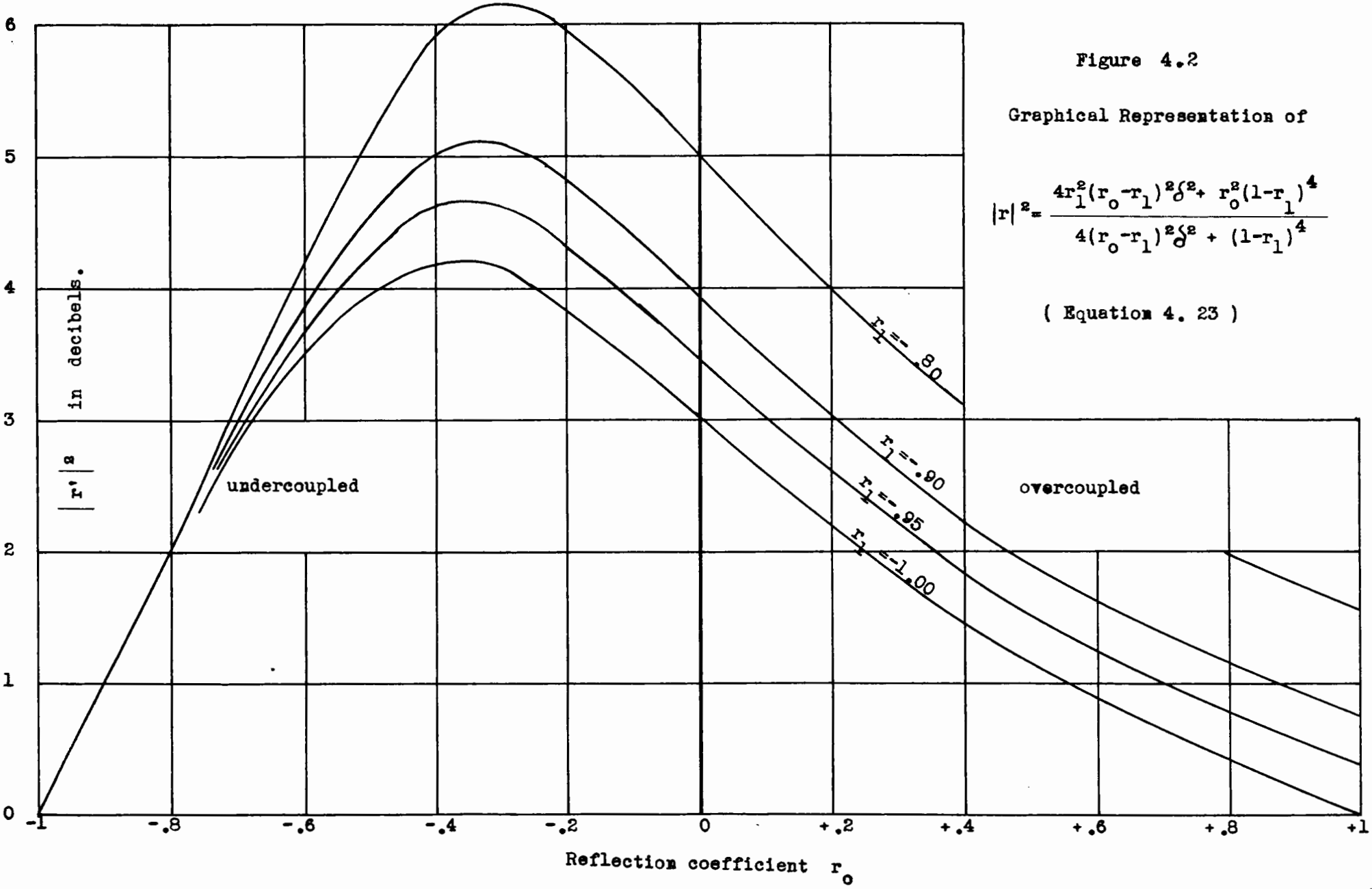

Figure 4.2

Graphical Representation of

$$|r|^2 = \frac{4r_1^2(r_o-r_1)^2\delta^2 + r_o^2(1-r_1)^4}{4(r_o-r_1)^2\delta^2 + (1-r_1)^4}$$

(Equation 4. 23)

greater the value of δ, the more closely $|r^1|^2$ approaches $|r_1|^2$ and the greater $2\Delta\omega$ becomes.

4.3 Determination of degree of coupling.

With reference to equation 4.9 and Figure 4.3, the degree of coupling may be ascertained by an investigation of the positions of the minima in the standing wave pattern on the input line. The reference points are the positions of the minima off resonance. The loop coupled resonator off resonance is equivalent to a short. If the resonator is under coupled, then at resonance $Q_E > Q_o$, so $R_o N^2 > R$, and $\frac{Z_{in}}{R_o} < 1$. Hence, the minima occur at the same points on the line as off resonance. If the resonator is overcoupled, then at resonance $Q_E < Q_o$, so $R_o N^2 < R$, and $\frac{Z_{in}}{R_o} > 1$. Hence, the minima are shifted by $\frac{\lambda}{4}$ from their positions off resonance.

The off-resonance positions of the minima are shifted slightly by the inductive loading of the loop, but the indication of the degree of coupling is very definite, even close to critical coupling.

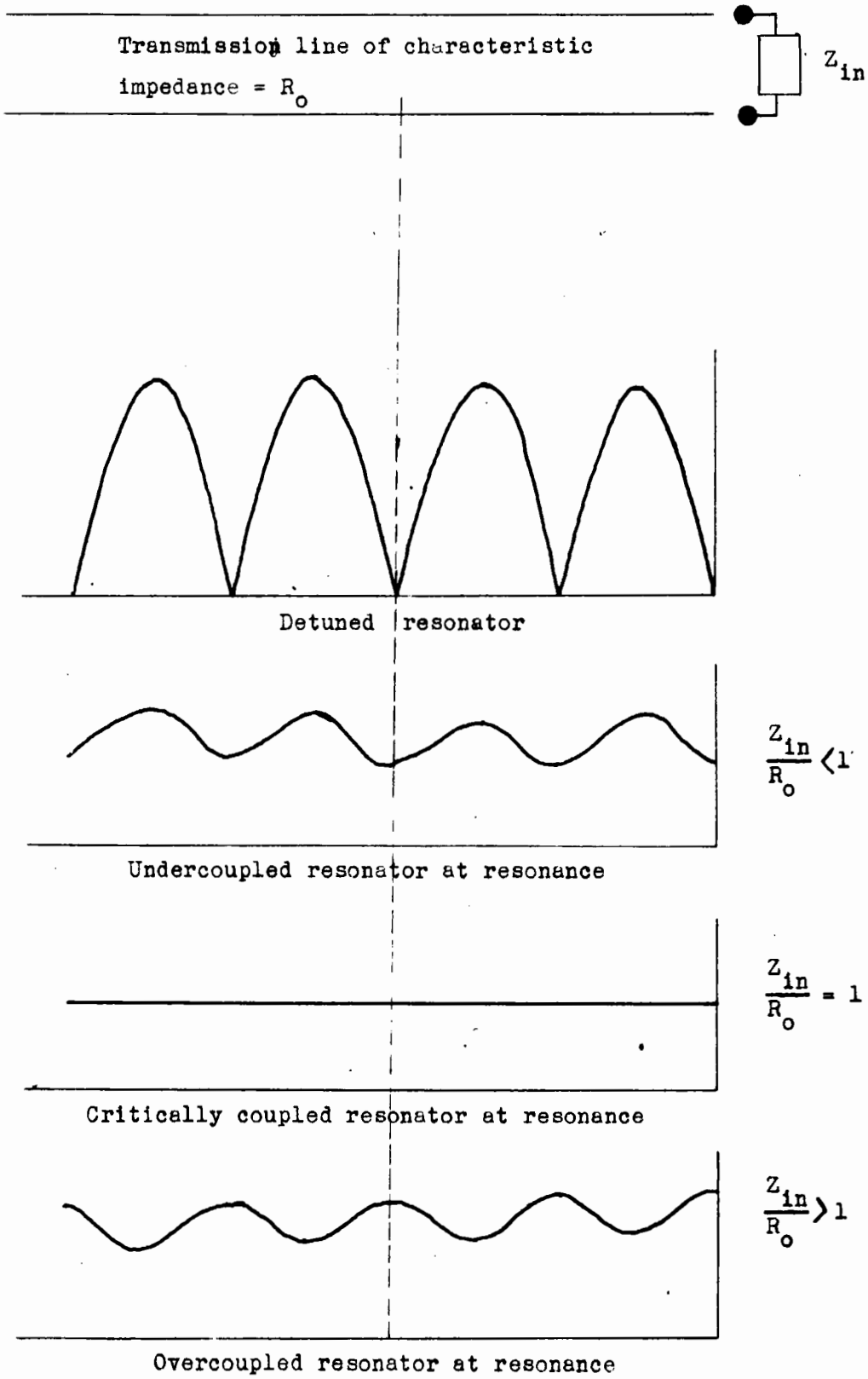

Figure 4.3 Standing wave patterns on the input line to a resonator for various degrees of coupling. Patterns shown are for loop coupling.

5. Experimental procedure.

From the discussion just completed, it is seen that if a method for measuring the reflection coefficient of the resonator as a function of frequency could be devised, its Q value could be determined.

There are at least two ways in which this can be accomplished. The first method is an alternate to the one used; and, since it has some advantages, might be considered for any further investigations in this field.

5.1 Alternate method.

If two directional couplers were placed "back-to-back" and the input connected to the main arm on one end and the resonator on the other end, then the voltage in the first coupler would be a measure of the incident power and the voltage in the second a measure of the reflected power. The reflection coefficient would be the ratio of the two outputs, suitably corrected for line losses and the decoupling in the couplers. The outputs (if from square law devices) would be proportional to the magnitude squared of the reflection coefficient, which is independent of the position of the termination in the waveguide, thus the phase shifts due to unequal path lengths could be ignored. If some circuit were available which would yield the quotient of the two outputs, then a meter

connected to this circuit could be calibrated to read directly in reflection coefficient. Such instruments are made commercially for frequency ranges other than the S band and are known as reflectometers.

A reflectometer of this type has the advantage over the method described below of involving components which are relatively insensitive to small frequency changes and require no matching devices in order to operate properly.

5.2 Procedure.

The method I have chosen is one originated by E.D. Reed of the Bell Telephone Laboratories.[9] This method is based on the fact that the output of a matched hybrid junction - a magic tee - depends only on the reflection coefficient of the termination on the test arm, if the other wide arm is terminated in a matched load. A sample of the incident power is taken from the input line through a directional coupler. The incident and reflected powers are displayed on alternate sweeps of a CRO. The power levels are made comparable through the use of variable attenuators and an initial condition set which is inherent in the apparatus.

The apparatus is shown schematically in Figure 5.1 and is described in the following chapter.

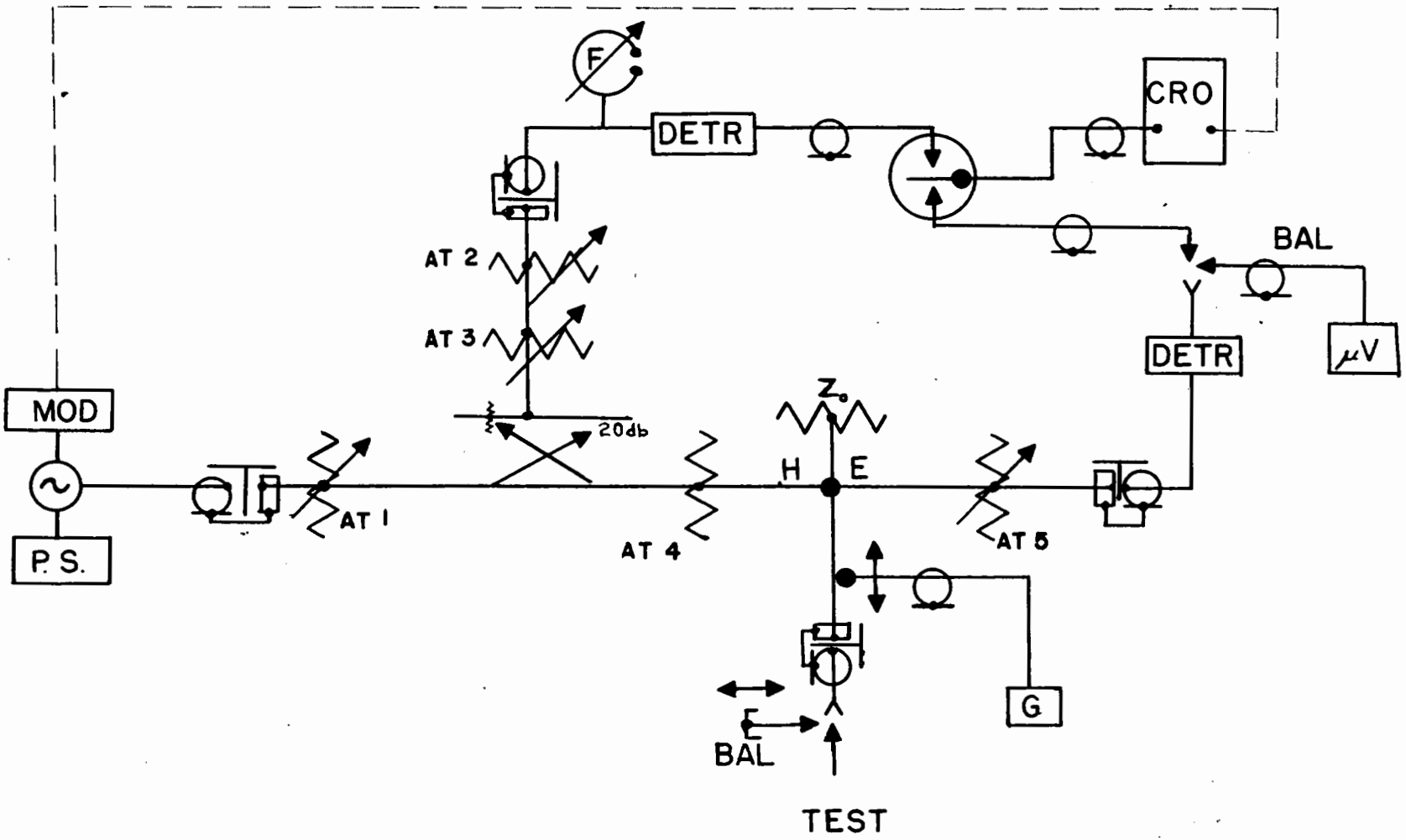

Figure 5.1 Schematic diagram of measurement apparatus.

Symbols as defined by: "Proc. I.R.E.,vol. 42,p 965."

The step by step procedure involved in the measurement of the Q of a resonant section was this:

1. The experimental section, mounted on a waveguide to coax adapter, was placed on the test arm of the tee.

2. The resonant frequency of the section was determined and marked by tuning the frequency meter to the resonant frequency. This was done while the source was being frequency-swept in order to minimize the hunting required to find the resonant frequency. The sweep was then turned off and the source operated on CW.

3. The test section was then replaced by a moveable short. The output of the tee was connected to a μvoltmeter and the slide-screw tuner adjusted until the reading of the μvoltmeter became independent of the position of the short. In this way the tee was matched.* The source was returned to sweep operation and the power levels of the two channels as indicated on the oscilloscope were made coincident by means of the variable attenuators in the channels.

4. The short was then replaced by the test section.

* See Appendix IV.

5. The degree of coupling to the resonant section was then determined by observing the position of the minima in the test arm (i.e., on the input line to the resonator) when the source was operated CW at resonance and then far removed from resonance. Far removed from resonance was that point closest to resonance at which the resonator had no noticeable effect on the reflected power.

6. $|r_1|^2$ and $|r_o|^2$ were then measured in terms of the micrometer setting of the precision attenuator, and recorded on a data form. These quantities were then found in decibels from the calibration curve of the attenuator.

7. From a conversion graph r_1 and r_o were found as algebraic ratios. The sign of r_o being assigned according to the degree of coupling.

8. The value of $|r'|^2$ was then determined from the plot of equation 4.23. If this resulted in the determination of $2\Delta f$ at an inconvenient power level, $|r'|^2$ was calculated for a more suitable value of δ. The attenuator setting corresponding to $|r'|^2$ was found from the calibration curve.

9. The bandwidth $2\Delta f$ was determined by reading the frequency meter dial settings for the points of intersection between the incident and reflected power

traces. These points were designated as f_1 above resonance and f_2 below. The dial setting for f_o was also observed and these quantities entered on the data sheet.

10. The appropriate corrections for temperature and calibration were made to the readings and the values of f_1, f_2 and f_o determined to two decimal places by the use of extended calibration curves.

11. Q_x, Q_E, and Q_o were then calculated.

Figure 5.2 shows a typical display. Step 6 is shown in Figures 5.3, 5.4 and step 9 in Figure 5.5. Plate 5.6 is a sample data form.

5.3 Although the steps listed above appear lengthy, many of them are the result of key components of the apparatus having calibration curves, rather than direct reading dials.

The method has all of the advantages that a sweep frequency method has over a point-to-point method plus some decided advantages over other sweep frequency methods.

The chief advantage of the system is that the effect of coupling changes are visible, predictable, and measurable. Coupling has emerged during the measurements as the prime factor determining convenience and

accuracy. The value as well as the sign of r_o are dependent on the amount of coupling and so the depth of the response curve of the resonator is dependent on coupling. The variation of r_o with coupling gives an indication of the degree of coupling and the amount of coupling.

Another advantage of the method is the absence of any amplifiers other than the oscilloscope, which is common to both channels. As long as the crystal detectors are identical, there are no other components which have to be matched. The system is independent of any amplitude modulation of the source because of the lack of amplifiers. The modulation need not be linear since the frequency axis of the display does not have to be calibrated.

The accuracy of the method is dependent on the matching of the tee and the likeness of the detectors. It also depends on the variation of the components with frequency, although the frequency variation for any one test is so small that it does not affect the accuracy. The tee has to remain matched over this small frequency difference, however. The match of the tee depends both on the frequency sensitivity of the tee and the slide screw tuner. It can only be assumed that this match holds for the frequency range of any one test.

Figure 5.2 A typical oscillographic display. The horizontal trace is the incident power, the small dip in it the wavemeter indication. The wider response curve is the reflected power.

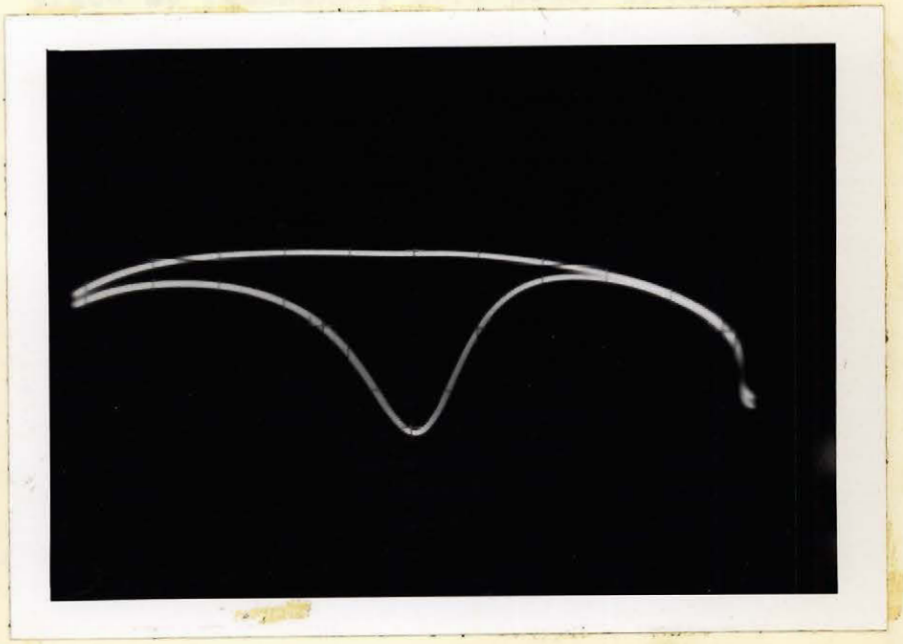

Figure 5.3 $|r_1|^2$ - Incident trace coincident with reflected trace off resonance.

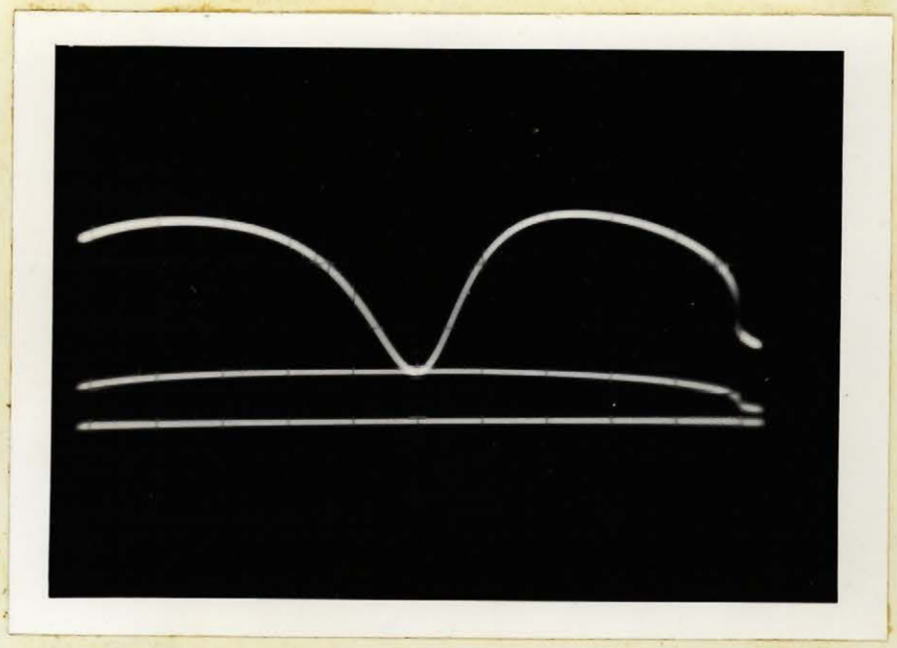

Figure 5.4 $|r_o|^2$ - Incident trace coincident with reflected trace at resonance. Zero power level shown.

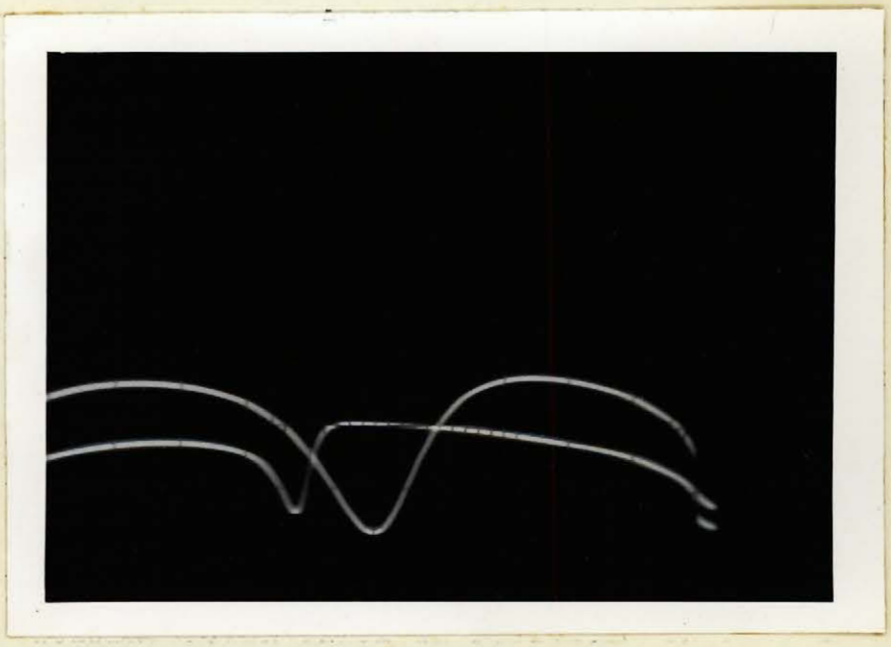

Figure 5.5 Incident power trace in position for bandwidth measurement.

Test:

d = 1/4" ; s = 1/2" ; = 8"

Date: June 24,1956.

ITEM	PRECISION ATT. SETTING	DB	REFLT COEFF	
$\|r_1\|^2$	93	0. 325	$r_1 = -$ 0. 960	OVERCOUPLED
$\|r_o\|^2$	436	7. 50	$r_o = +$ 0. 420	TEMPERATURE = 25. 8° C
$\|r'\|^2$	300	3. 66		

$(1 - r_1)$	$(1 - r_o)$	$(1-r_1)(1-r_o)$	$(r_o - r_1)$	$2(r_o - r_1)$	$\frac{2(r_o - r_1)}{(1-r_1)(1-r_o)}$
1. 960	0. 580	1. 137	1. 380	2. 760	Q_x = 2. 427

ITEM	f_1	f_2	f_o
Dial setting D	3. 0306	3. 0242	3. 0274
Temp. correction K	+ 0. 0001	+ 0. 0001	+ 0. 0001
R'=D+K	3. 0307	3. 0243	3. 0275
Dev. correction d	+ 0. 0001	+ 0. 0001	+ 0. 0001
Corrected setting R (R=R'+d)	3. 0308	3. 0244	3. 0276
f_{int}	2947. 40	2950. 12	2948. 76
Hum. correction $1 + \frac{\Delta f}{100}$	-	-	-
$f = f_{int}(1 + \frac{\Delta f}{100})$	-	-	-
$2\Delta f$	2. 72		f_o = 2948. 76
$Q_E = \frac{(f_o)}{(2\Delta f)}$	1084		
Q_x	2. 427		
$Q_o = Q_x \cdot Q_E$	2631		

r'^2 has been calculated for = 1.

Humidity corrections have been neglected.

Figure 5.6 A typical data form.

Figure 5.6

The detectors must have the same input-output characteristics or the difference in power between reflected and incident channels, as indicated by the position of the traces, will be caused in part by the detectors rather than the resonator. The crystal matching is described in the following chapter. If the tee is well and truly matched then the only possible source of error in the apparatus is the detectors. An error of approximately 0.5%, caused by the humidity of the air in the frequency meter, has been allowed.

The disadvantages of the Reed method which became apparent durihg the tests were in the most part the fault of the apparatus used. In the first place, the hybrid junction requires matched generator and load to operate as a magic tee, and this matching is very frequency sensitive and adds a great deal of labour to the tests. It would be ideal for fixed frequency operation. However, in these tests the resonant frequencies of the various sections were not identical and hence the matching had to be done for each new section. Secondly, the display on the face of the 'scope is the power versus reflector voltage characteristic of the klystron and is of the familiar klystron mode shape. The tuning range of the 2K41 is very limited and hence the edges of the response curve often reached the edges of the klystron mode. This would not have occurred if the resonators had had Q's two or three times as large as they did. When the response cur-

ve was very wide it made the determination of r_1 difficult. r_1 was usually found by detuning the resonator by placing a block of brass near the coupling loop, so that the currents flowing through the loop would be the coupling system currents only. A third disadvantage was the many steps involved in obtaining a final result. As mentioned above, this could have been eliminated by using equipment which was calibrated directly rather than through curves.

Aside from the above mentioned disadvantages, the method used is convenient and shows the processes involved very graphically.

6. Apparatus.

6.1 Apparatus in general.

The apparatus in general consists of a source of 10 cm energy, a waveguide transmission system, detectors, a switching SPDT relay and an oscilloscope. The source and oscilloscope are swept by a 120 cycle sawtooth wave, such that the switch inputs are displayed on alternate sweeps, and each is representative of the same portion of the source characteristic. (Figure 5.1)

The energy is fed from the source through a variable attenuator to a directional coupler. The low level output of the coupler is passed through a variable attenuator, a calibrated attenuator, and a frequency meter to a crystal detector. The signal from this detector is applied to one side of the switching relay. The high level output of the directional coupler is fed through a 10db pad and a slide screw tuner to the H arm of a hybrid tee. One side arm of the tee is terminated in a flat load and the test piece is placed on the other. The output of the E arm of the tee is passed through a variable attenuator to a crystal detector. This signal is applied to the other side of the switching relay. The center contact of the relay is connected to the vertical amplifier of the oscilloscope.

6.2 The Apparatus in Particular.

6.2.1 The signal source used was a 2K41 reflex klystron. This klystron is also known as the 417A. The 2K41 has a minimum power output of 250 milliwatts within the published frequency range of 2660 to 3310 Mc/s. In practice it was found that the klystron operated well beyond these limits.

The klystron was operated under the following conditions:

Beam voltage	.....	-1000 volts
Reflector voltage	.....	-50 to -600 volts
Grid voltage	.....	-30 volts
Beam current	.....	40 to 50 milliamps

The klystron could have been operated at a higher beam voltage if more power were desired. However, the electronic tuning bandwidth of the 2K41 is very limited and decreases as the beam voltage is increased. It was also found to have severe electronic tuning hysteresis. The tuning bandwidth is of the order of 5 to 10 Mc/s under the above operating conditions.

The klystron was mounted on a small Hammond chassis and was air cooled by a fan mounted on the same chassis. The modulation coupling condensers were also mounted on this chassis. (Figure 6.1)

A typical mode is shown in Figure 6.1A. The voltage increases negatively to the right. The multiple-transit effect is shown by the steps.

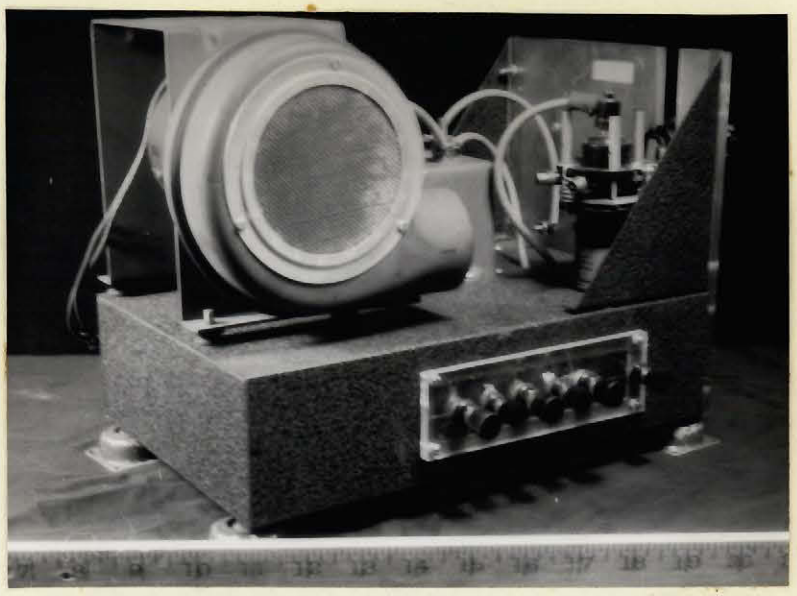

Figure 6.1 2K41 Klystron and fan.

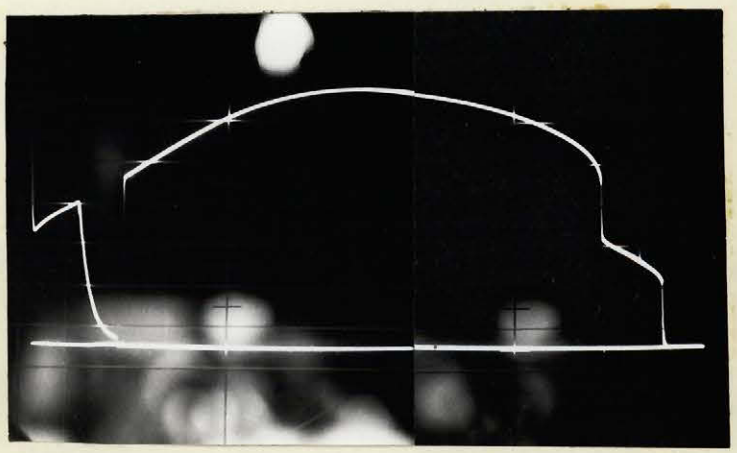

Figure 6.1A Typical mode of 2K41 Klystron. Pout vs. Reflector.

6.2.2 The klystron power supply (Figure 6.3) was a home-made version of the PRD 801 Universal Klystron Power Supply, built in the Department some years ago. It is capable of delivering approximately 80 milliamperes of current from -300 to -3500 volts, with appropriate reflector voltages. It has grid voltages available from +40 volts to -200 volts. Since this supply had no modulation source, it was necessary to construct a sweep generator. Because of the tuning hysteresis of the klystron, the sweep had to be a sawtooth waveform which would vary the reflector voltage in one direction only. The frequency of the sweep had to be 120 cps since it had to occur once while the switching relay was in each position, i.e., it had to sweep once for each half cycle of the 60 cycle-relay drive. In order to obtain a frequency range sufficiently larger than the bandwidth of the resonant sections it was necessary to sweep almost the entire mode of the klystron. This required a sweep voltage amplitude of about 100 volts.

To insure that the sweep frequency was exactly half of the switching frequency, the sweep was synchronized to the line voltage. This was accomplished by applying the pulses from an inverted and clipped full-wave-rectified line signal to the grid of the 884 thyratron which acted as the sweep generator. The sweep generator is shown in Figure 6.4. The phase shift introduced between

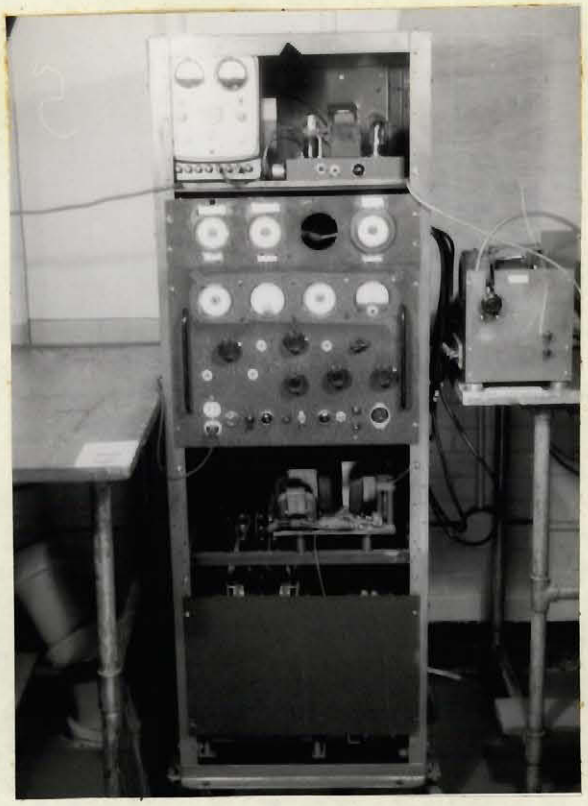

Figure 6.2 Klystron Power Supply

Figure 6.3 60 cycle Switching Relay , showing BNC connectors.

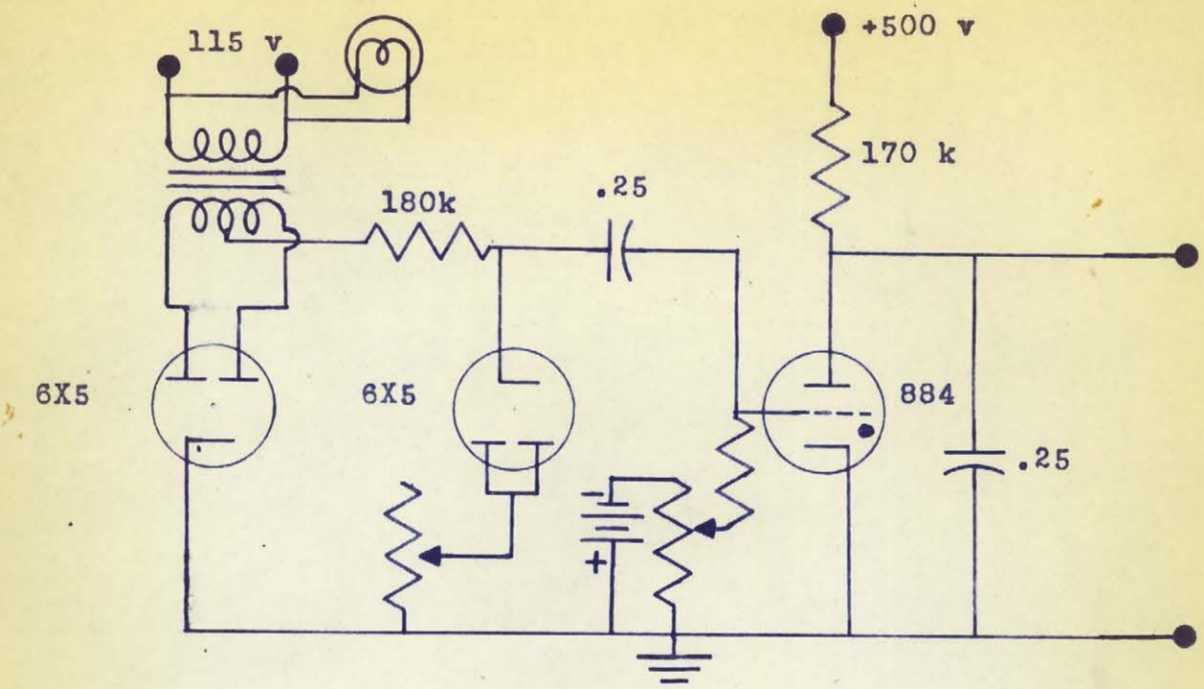

Schematic circuit diagram.

View of assembled chassis.

Figure 6.4 Synchronized, saw-tooth sweep generator.

the sweep and the switching caused the switching transient to appear away from the edges of the display on the oscilloscope. This transient is shown on the left side of the display in Figure 6.1A.

The switching relay was a Stevens-Arnold DC-AC chopper (type C-12, 60 cycle). The chopper was driven by the 6.3 volt side of a Hammond 1128X60 transformer. An off-on switch was placed in the line side of the transformer. The inputs and the output of the switch were made through BNC (type UG 290/U) connectors. The relay was mounted on a chassis and all 60 cps leads were shielded to minimize stray pickup. (Figure 6.3)

6.2.3 The waveguide circuitry was composed of standard Hewlett Packard S band components, except for the slide screw tuner. Views of the apparatus are shown in Figures 6.5 to 6.8. The S band waveguide is 3" x 1½" outside dimensions and has a suggested bandwidth of 2.6 to 3.95 KMc/s. It is electroplated on the inner surfaces with a high conductivity bright alloy. Connections are made between sections by means of flat flanges, type UG-53/U. The transitions between coax and waveguide are made through S281A waveguide-to-coaxial adapters; the coaxial fitting is N type. The klystron was connected to the waveguide through a short length of RG 8/U coaxial cable, fitted with N type connectors.

The variable attenuators are of the flap type. They have an attenuation range of 0 to 20 db and calibration curves are supplied. An interesting feature is that the flap enters the guide linearly rather than pivoting in. This tends to minimize the SWR. The precision,calibrated, attenuator has a range of attenuation of 0 to 20 db, however, the calibration extends for only 10 db. The resistive material is deposited on a card which is moved laterally across the guide by the action of a micrometer screw. The micrometer is graduated in inches and to obtain the attenuation in decibels it is necessary to refer to a calibration curve. Since the device is frequency sensitive the calibration is good only at that frequency at which it was done. The particular attenuator used was calibrated at 3000 Mc/s. The calibration accuracy is 0.3 db.

The directional coupler (S752D) has 20 db attenuation between the main and side arms. It is of the multihole type.

The hybrid tee (S845A) is a matched four arm junction. There are no matching posts nor irses in the tee, which is the usual method of matching hybrid junctions. The catalogue description of the component describes it as being matched by careful choice of dimensions. In practice it was found necessary to match the input arm by means of a slide-screw tuner. This tuner consisted of a

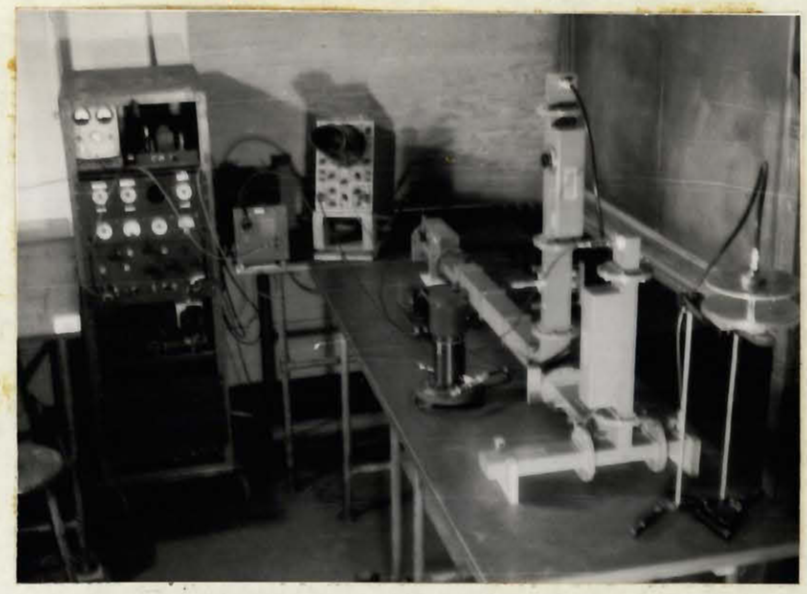

Figure 6.5 Apparatus - showing original waveguide circuitry - no tuner, slotted line, or isolating lengths. Coupling system as originally used.

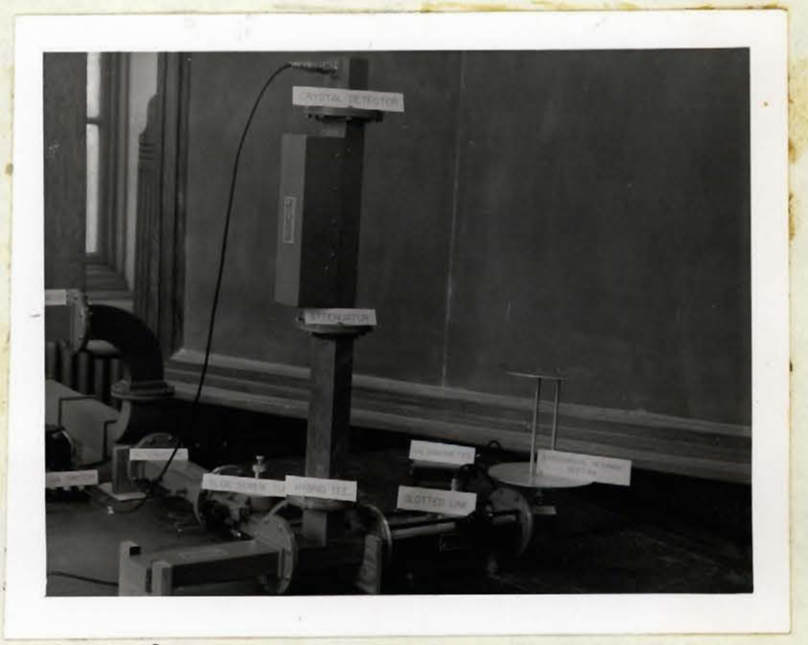

Figure 6.6 Final Equipment Layout - vicinity of magic tee.

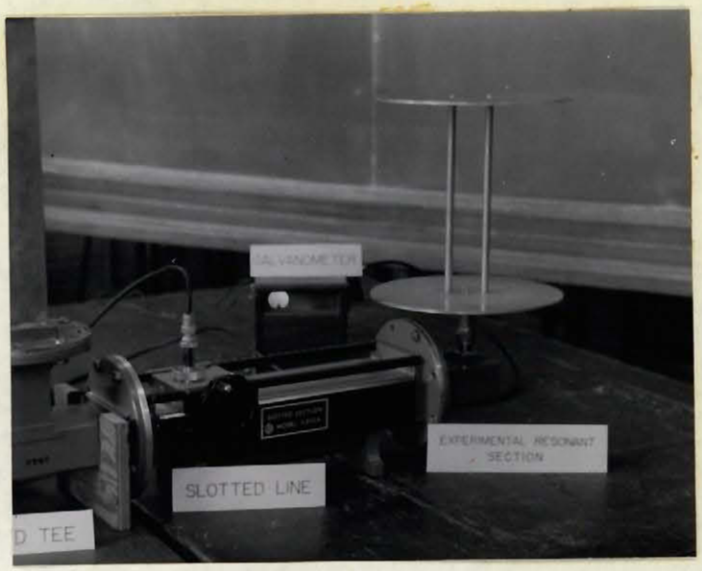

Figure 6.7 Close-up of Resonator - connected to apparatus.

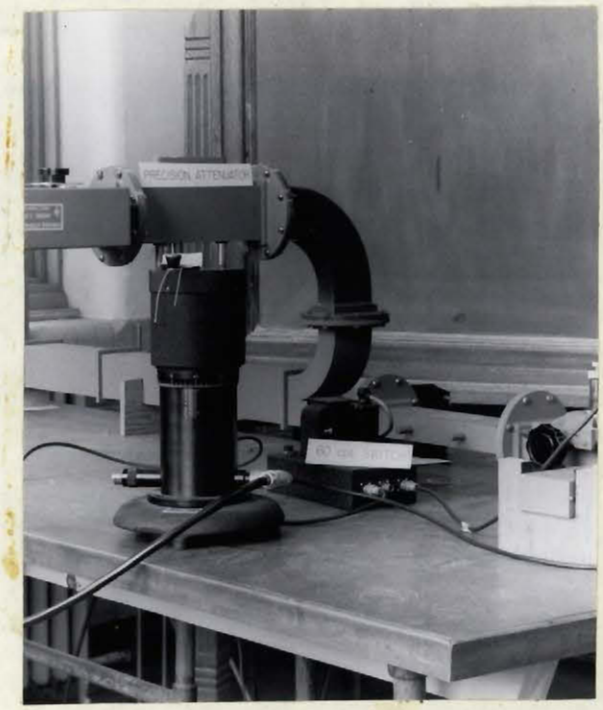

Figure 6.8 Frequency meter and Switching Relay.

6-32 screw inserted into a length of guide through a slot milled in a broad face. The position and insertion depth of the screw could be varied, and hence most susceptances obtained. When the other arms of the tee were terminated in mis-matched components, modes other than the TE_{10} were excited in these arms and coupled to the input arm. Since the tuner was effective in matching only the dominant mode it was found to be necessary to decouple the components on the other arms from the tee, by lengths of waveguide. In this way the spurious modes caused by the mis-matches were attenuated to a negligible value before reaching the tee. The variable flap attenuator on the E arm of the tee was decoupled with a 12" length of straight waveguide. The reference side arm of the tee was terminated in a low power non-reflective termination (S910A). The test piece was decoupled with a S810A slotted section. Since the determination of the degree of coupling depends on a knowledge of the SWR on the input line to the test piece, the insertion of the slotted section served both purposes. This is an addition to the equipment used by Reed, and a very convenient one, since the degree of coupling could be readily determined at any time. The output of the 444A untuned probe on the slotted section was indicated on a Leeds and Northrup 2420B galvanometer.

The moveable (S920A) short used to match the tee consisted of a screw driven silvered plate which made contact with the walls of the guide through spring fingers. Its loss is reported to be less than 0.01 db in excess of a silver plated soldered short, even after 25,000 tuning cycles. When the tee was being matched, the output of the E arm was measured on a Weston 322 μvoltmeter, as indicated by the symbol BAL on Figure 5.1.

The output of the incident power channel was fed through a waveguide to coax adapter, through a length of RG 8/U to a coaxial tee. The Sperry 291A Microline frequency meter was connected directly to the side arm of this tee. It was operated as an absorption cavity and hence its resonance was indicated by a drop in the power level in the main channel. The straight-through side of the tee was connected to a crystal detector.

6.2.4 The detectors were IN23 crystals mounted in PRD 613M crystal mounts. These mounts are coaxial and have an N type fitting on the RF side and a BNC fitting on the DC side. As has been mentioned previously, the accuracy of the measurements depends on the crystals being identical. That is, their output versus input characteristics should be the same over the range of input power used. This response can be readily checked when the short is in position on the hybrid tee. After the tee is matched and the short still in place, the output of the tee

is dependent only on the input. So, if the incident and reflected traces are made coincident on the scope by adjusting AT 2 and AT 5 and the input power varied by attenuator 1, the response of the two crystals may be compared by observing their output levels on the scope. If the traces remain coincident, as AT 1 is varied, then the crystals may be considered identical. Several crystals were compared in this manner until a pair whose responses were the same was found. The crystals were paired by first measuring their parameters with a crystal checker, so as to eliminate crystals which were radically different. The pair finally chosen agreed within 0.1 db. Originally H-P crystal detectors were used. These detectors employed coaxial IN26 crystals, modified to fit the mounts. One of these crystals failed, and since they are rare compared to the common IN23's and must be ordered from the manufacturer, the PRD mounts were substituted. Also, in order to find a matched pair, many crystals were tried and the IN26's were in too short a supply to find a matched pair.

The experimental resonators were mounted on the coaxial fitting of a waveguide to coax adapter placed on the end of the slotted section. Originally, they had been coupled to the adapter through a short length of coaxial cable but this was done away with through a process of evolution. The original coupling system is illus-

trated in Figure 6.5, and the final one in Figures 6.6 and 6.7.

6.3 Experimental resonant sections.

The sections of parallel wire transmission line whose Q's were measured consisted of the parallel cylindrical conductors, the terminations, and a coupling circuit. The resonators are shown in Figures 6.9, 6.10 and 6.11.

6.3.1 Conductors.

The conductors were constructed from lengths of pure silver tubing, the ends of which were pressed fitted with brass plugs. These plugs were soldered within the tubing; and drilled and tapped to take 4-40 screws. The ends of the conductors were turned slightly concave so that only the outer edge made contact with the termination. This was to insure that the dimensions of the conductors would be known at the point of contact and to make the mechanical contact as good as possible. The absolute length of the conductors was not specified critically. However, the two conductors of any one pair were machined to within one thousand of an inch of each other. Conductors of the following dimensions were made:

TABLE II

d	ℓ
$\frac{1}{4}$	2", 4", 6", and 8".
5/16	2", 4", 6", and 8".
0.54	2", 4", and 6".
3/16 x 5/8 rect.	2" and 4".

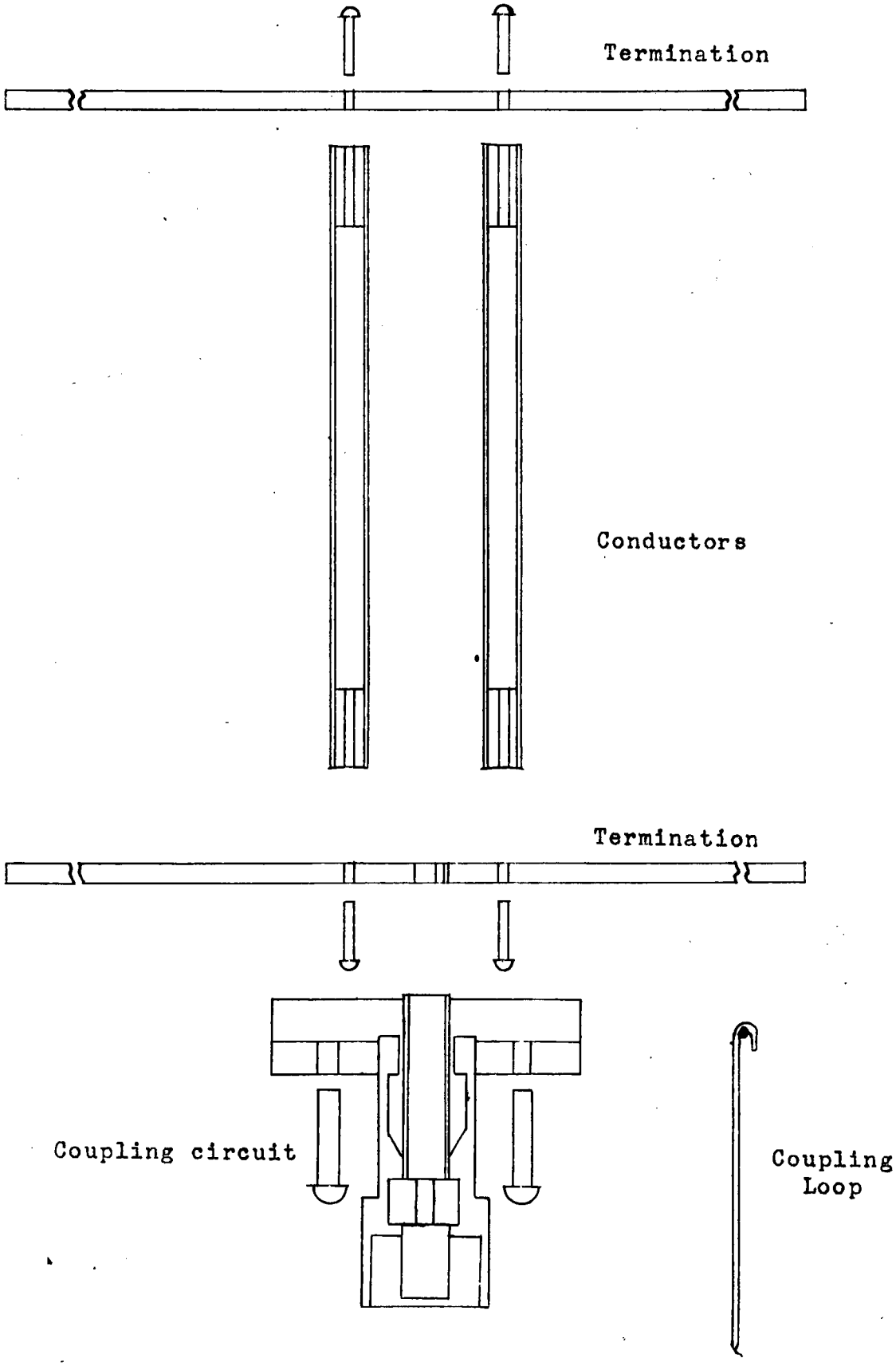

Figure 6.9 Exploded cross section of experimental resonant section. Full size except as indicated.

Figure 6.10 Assembled Resonator.

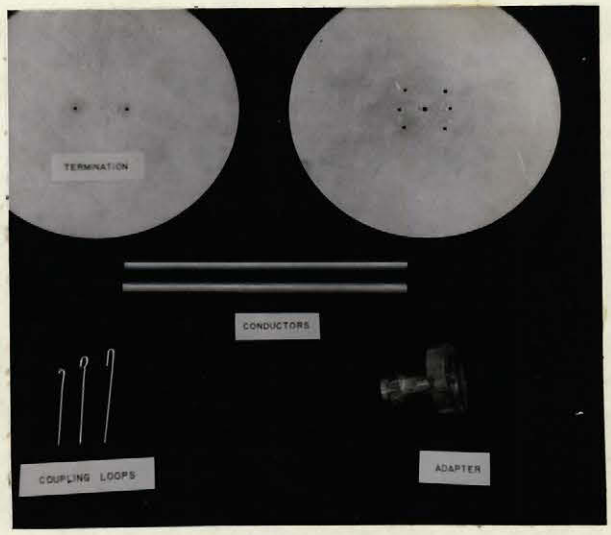

Figure 6.11 Components of Resonator.

Other conductors were tried as the situation warranted.

6.3.2 Terminations.

The terminations were 8" diameter, circular discs, cut from 1/8th inch brass stock. Originally, the terminations had consisted of a single pair of 8" discs, with slots milled in them to allow for different conductor spacings. It was felt that these slots would interfer with the fields at the terminations, since in many cases they would lie within the half-power circle. And so they were replaced by four pairs of terminations, each pair to serve as the terminations for a different conductor spacing. Two holes were drilled in each disc to pass the 4-40 screws with which the conductors were held secure. Allowance was made for conductor separations of $\frac{1}{2}$", 1", $1\frac{1}{2}$" and 2". The edges of the discs were turned in a lathe to make the discs truly round but the faces were left as-is. The conducting surfaces of the terminations were silverplated to a depth greater than the skin depth in silver at 3000 Mc/s.

The termination on the coupling end of the resonator had four 6-32 tapped holes symmetrically placed about the center to receive the coupling circuit. This disc has a one-eighth diameter hole at its center to allow insertion of the coupling loop into the resonator. A 0.059" diameter hole was drilled as near as possible to the cen-

ter hole, and on the line joining the centers of the conductors, to receive one end of the coupling loop. These details are shown in Figure 6.11.

6.3.3 Coupling Circuit.

The coupling circuit consisted of the outer conductor of a UG 21B, N-type coaxial cable connector and a circular brass block. The connector is in two pieces. The longer piece has the N type fitting at one end and the other end is threaded to screw onto the shorter piece. The shorter piece of the cable connector is soldered into the block. A piece of silver tubing is press-fitted into the center of the longer piece and when the connector is screwed together this tubing protrudes beyond the end of the block about 0.003". The protruding tubing insures a tight contact between the coupling system and the termination. The block is held to the back of the termination disc by means of four 6-32 screws, which mate with the holes in the termination. These screws penetrate the termination so that, when tight, their ends are flush with the conducting surface of the termination. The brass block has been heavily silver plated. A $\frac{1}{4}$" wide slot has been milled in the surface of the block to provide clearance for the heads of the screws which hold the conductors in place. These construction details are shown quite

well in Figure 6.11 where the coupling circuit is labled "ADAPTER". When the coupling circuit is connected to the assembled resonator the whole structure is connected directly to the female N type fitting of a waveguide to coax adapter, which is then placed in position at the end of the slotted section.

The coupling loop was made of 0.060" silver rod. A suitable length, pointed at one end to fit the center conductor of the fitting on the adapter and hooked at the other to form the loop, was placed in position after the block was affixed to the termination. The end of the loop was pressed into the 0.059" hole in the termination and, hence, a good mechanical joint made at the surface of the termination. The degree of coupling was changed by varying the loop insertion.

The coupling system described above evolved from a more complex one. The original coupling consisted of the same block fitted with a female N type receptacle. The coupling loop passed from the center conductor of this receptacle through the center hole in the termination, returned, and was soldered to the block. The resonator was then connected to the waveguide-to-coax adapter by means of a short length of RG 8/U coaxial cable. The degree of coupling was varied by rotating the loop with respect to the plane of the conductors. This led to frequent breakages in loops and ambiguity in

the coupling, i.e., it was often hard totell whether or not the coupling was to the transmission line mode and whether the coupling was loop or probe coupling. It was by varying the length of the connecting coaxial line that the effect of the hybrid tee mis-match was seen to be important, since the zero level set depended on the length between the tee and the short, and hence the impedance seen by the tee. A GR sexless connector was fitted to the end of a piece of RG 8/U having an N type at the other end and a GR shorting element used when setting the zero level.

7 Results and Conclusions.

7.1 Results.

The results of some fifty tests were considered valid. Approximately seventy others were invalidated by apparatus mis-matches. The invalid tests, however, were of the same magnitude as the final results and indicate that the final results are correct.

Three sets of results are presented.

1. The first set of results constitutes the bulk of the measurements. These tests demonstrate the Q values obtainable with the experimental resonant sections.

   The Q factor has been plotted as a function of length for three conductor diameters in Figures 7.1, 7.2, and 7.3.

   Using these results and Equation 2.25, values of R_{rad} have been calculated for each case. R_{rad} has then been plotted on a log-log graph as a function of $(\frac{s}{\lambda})^2 \ell$. This plot (Figure 7.4) is a straight line with a slope of 1, indicating that R_{rad} varies directly as $(\frac{s}{\lambda})^2 \ell$.

2. The second set of results was taken to illustrate the effect of conductor losses on the Q factors. Values were found for brass conductors, 4" in

length, at separations of ½", 1", and 1½". These conductors were then silverplated, and theQ's re-measured.

TABLE III

s	Q					
	Brass			Silver		
	Calc.	Emp.	Dev.	Calc.	Emp.	Dev.
1½"	985	908	-8%	1065	942	-11%
1"	1420	1318	-7%	1630	1404	-14%
½"	1810	1618	-10%	2515	2258	-10%

The calculated values were obtained from Figure I.3 used in conjunction with equation 2.25.
The empirical results are consistently lower than the calculated values, indicating that the radiation is dependent on the physical condition of the conductor surfaces. The silver tubing used during the first tests was smooth surfaced, whereas the brass rod used in these tests was comparatively rough. The silverplating was unpolished and very rough.

3. The third set of results replaced the tests on the shielded line, and were intended as a check on the method. They were made on a right circular cavity, oscillating in the TM_{012} mode. This cavity was used by K.J.Keeping and is described in his Ph.D. thesis (McGill,1952).

It is a precision device, tunable, and 10.419 cms. in diameter. It is made of two cup-like sections which mate (presumably) at a current node on the side walls. The conducting surfaces are heavily silverplated.

Results were obtained for both loop and probe coupling to this cavity. To loop couple to the TM_{012} mode is a problem. It requires an off-center loop and it was found that even with a loop of maximum dimensions (one half wavelength by the radius) the coupling was inefficient. Coupling to other modes was evidenced by the observation of resonances other than the TM_{012} resonance. The derivation of Appendix II was necessitated by this poor coupling. Therefore, the results of the loop coupled tests are included for contrast only. They include some results taken before the apparatus reached its final stage of sophistication.

The results, since they did not agree with the calculated value (Table I) were checked by the "Cold Test" method. The resonance curve obtained during this test is shown in Figure 7.5.

The results may be tabulated:

	Probe	Loop	VSWR
	10612	9176	10390
	10802	10545	
	10590	13386	
	10767	13040	
		11535	
		12434	
		11427	
Average	10692	11649	10390

Notice the small variations in the values of the probe coupled results as compared to the loop coupled results.

The deviation between the probe-coupled and VSWR results is less than 2%.

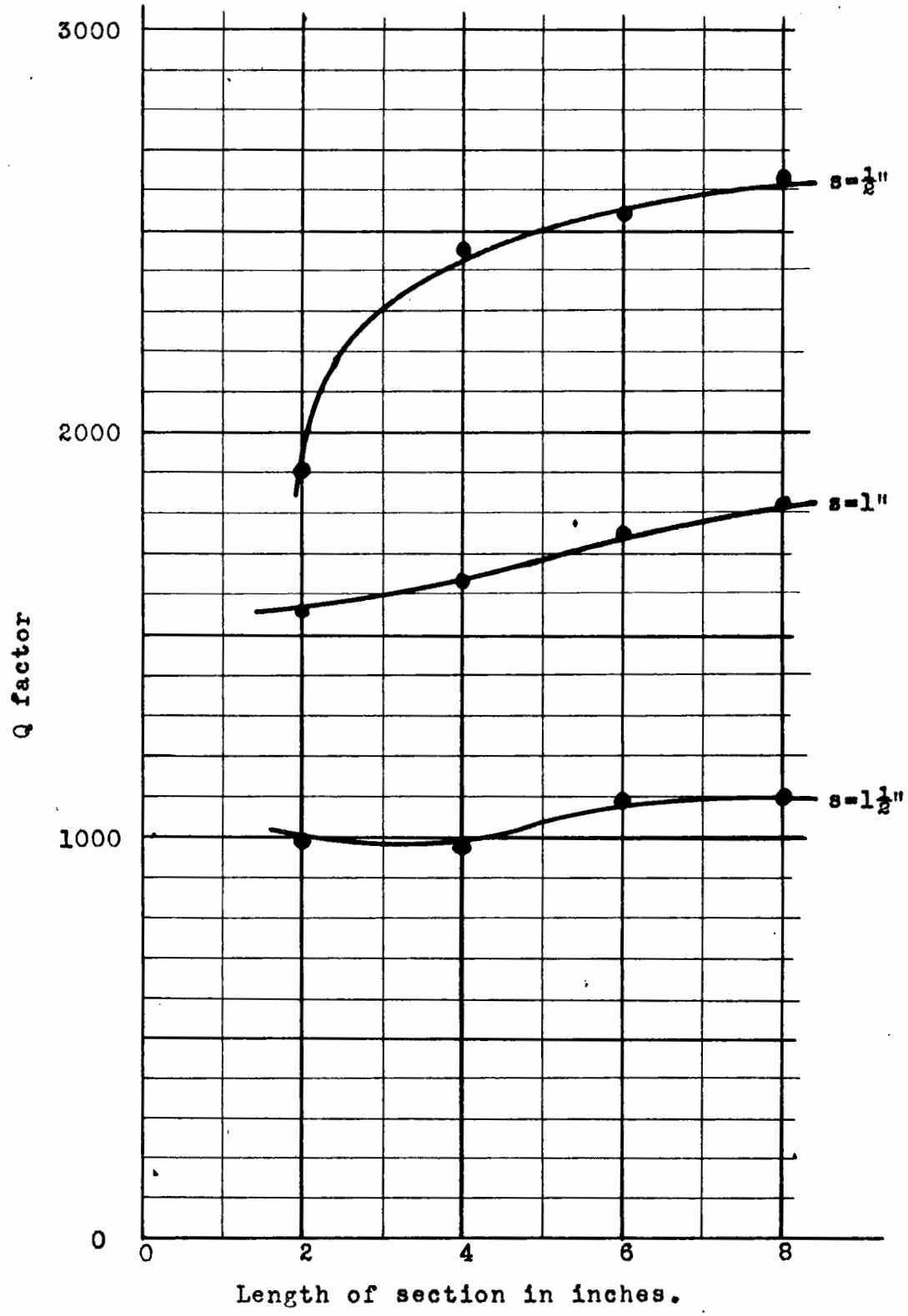

Figure 7.1 Experimental variation of Q with length.
Conductor diameter = ¼".

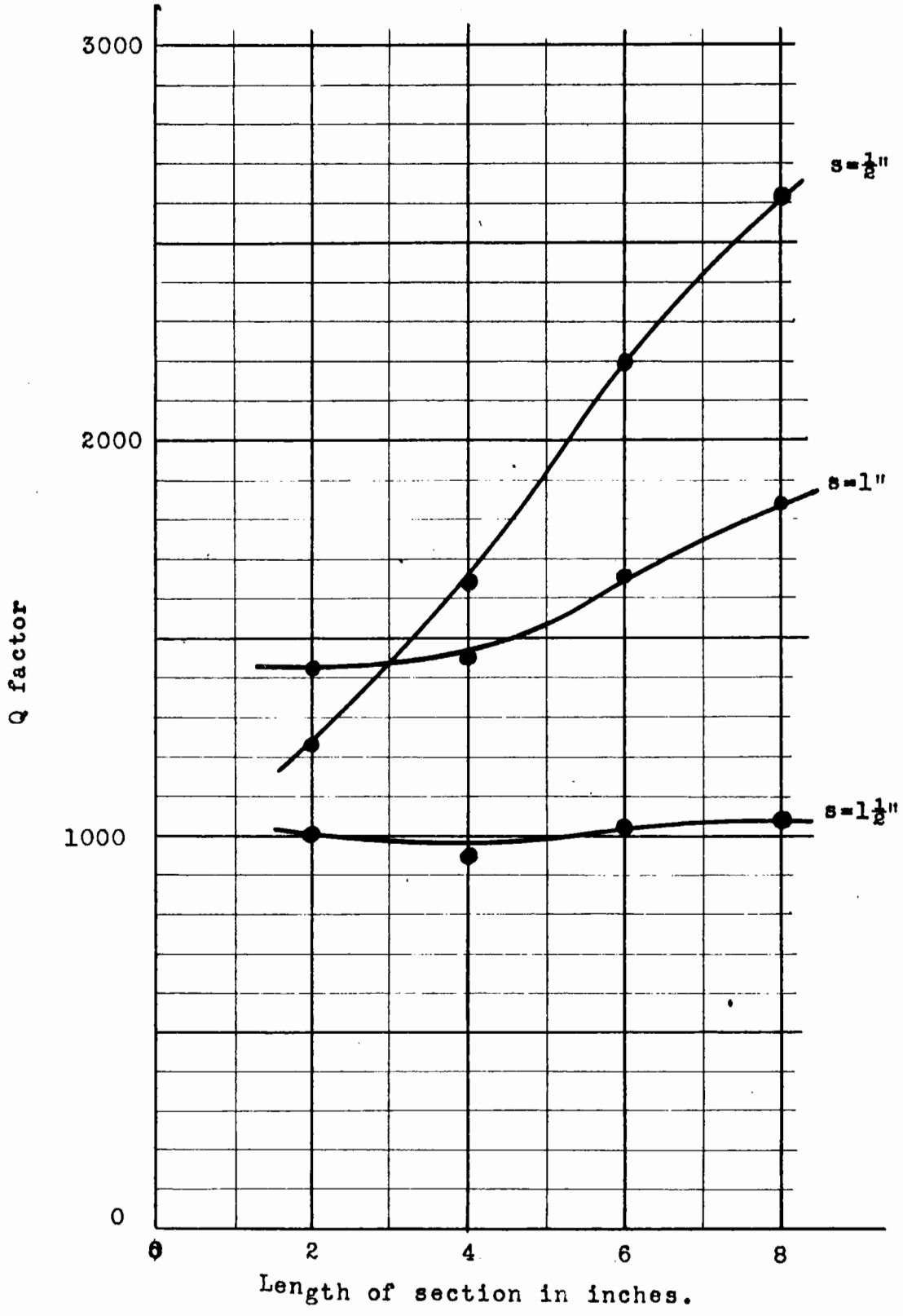

Figure 7.2 Experimental variation of Q with length.
Conductor diameter = 5/16".

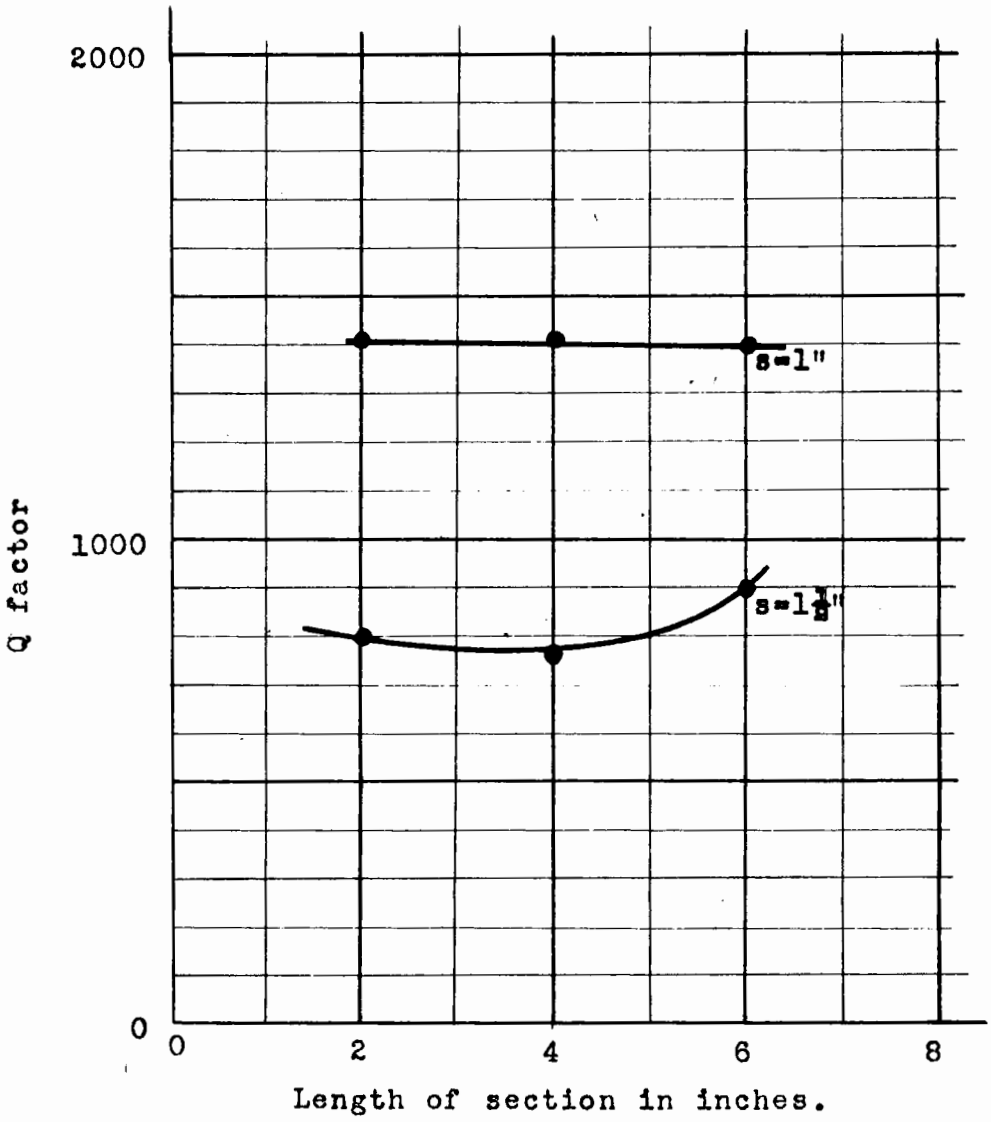

Figure 7.3 Experimental variation of Q with length.
Conductor diameter = 0.540".

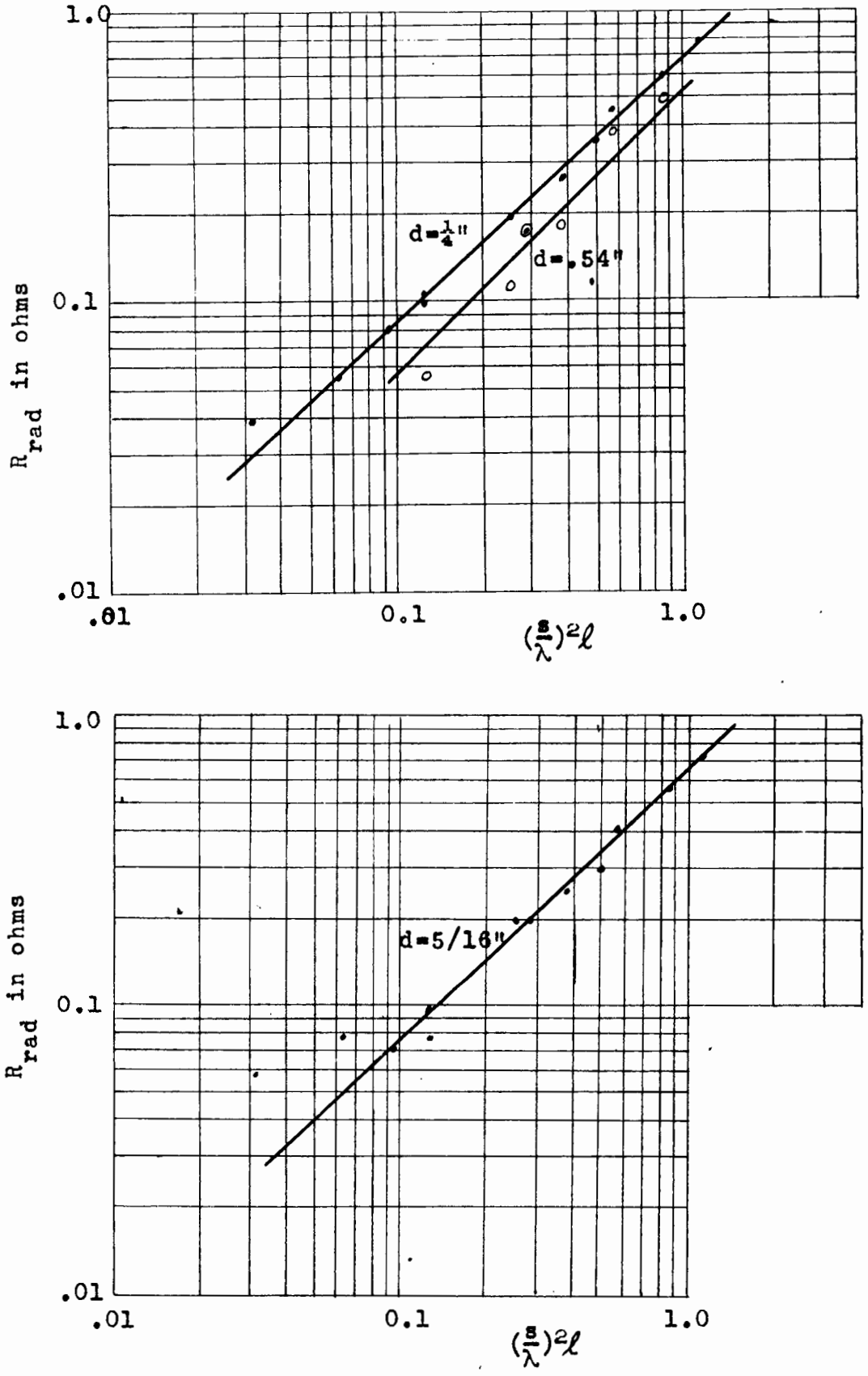

Figure7.4. Radiation resistance as a function of $(\frac{s}{\lambda})^2\ell$.

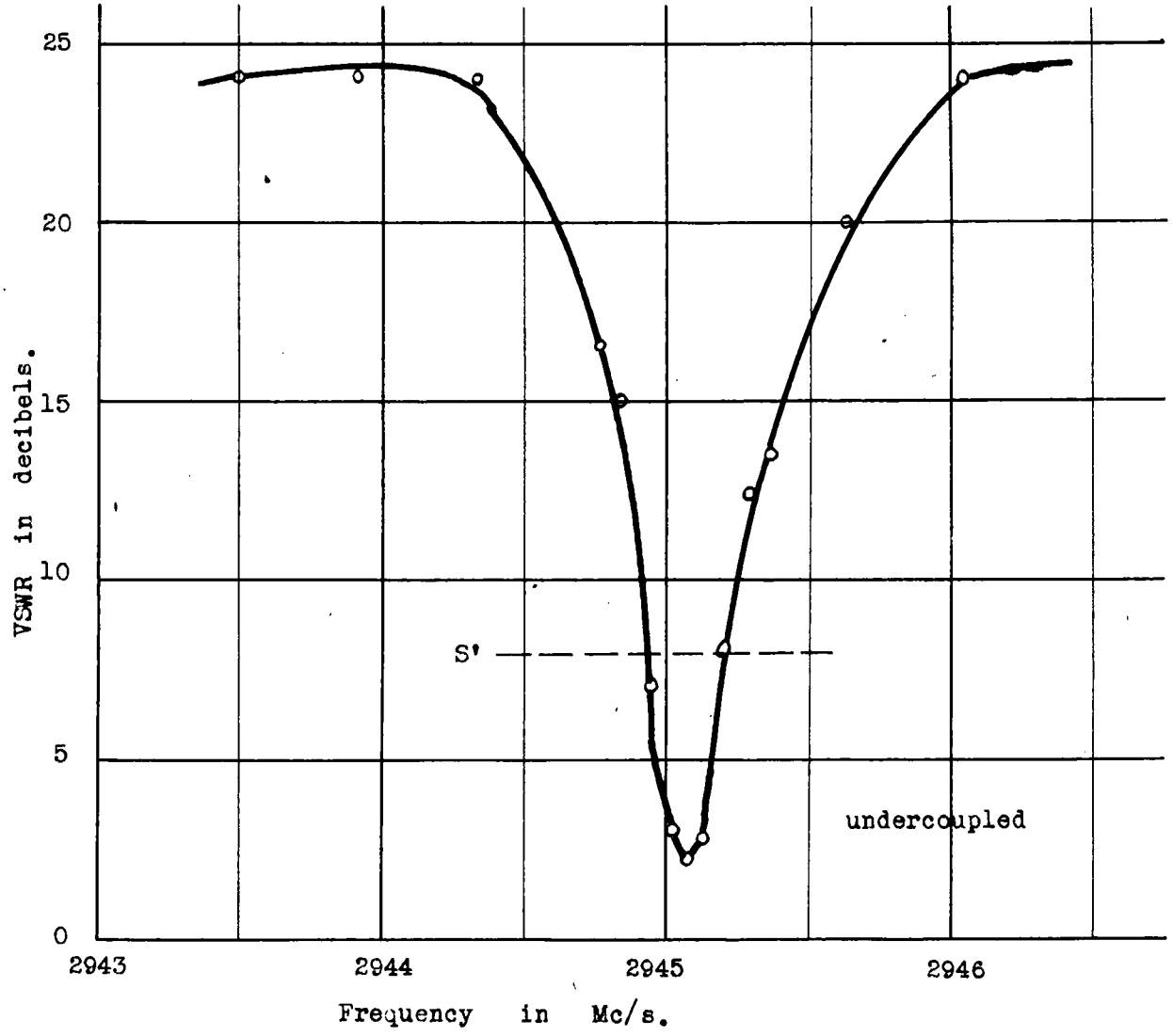

Figure 7.5 TM_{012} Cavity. VSWR versus frequency.

By the cold test method:

S_1 = 24 db

S_0 = 2.2 db

S' = 8 db

f = 0.27 Mc/s

f_0 = 2945.06 Mc/s

Q_0 = 10390

Q_E = 14550

7.2 Conclusions.

1. The first conclusion that may be made is that the method is satisfactory and convenient. However, its greatest value lies in the graphic way it illustrates the processes involved - the coupling, loading, and resonance, of the resonator.

2. The results are consistent and the error is estimated at $\pm 3\%$. A great deal of this error is introduced by the many graphs which must be read to obtain a final result. It is fortunate that a large deviation on one graph often resulted in a negligible error on the next graph. This way the errors tended to cancel rather than accumulate.

3. The agreement between the Reed method and the VSWR measurements on the TM_{012} cavity is indeed gratifying. The discrepancy between the empirical and the calculated result could be attributed to improper dimensioning of the cavity; i.e., the joint between the sections might not occur at a current null, and hence introduce an unexpected loss into the cavity.

4. The highest Q's were obtained with small conductors at small separation, of sufficient length to overcome the termination losses.

If the diameter of the conductors is made small the conductor losses become prohibitive, the termination and radiation losses increase. However, the energy storage also increases and the Q increases slightly.

If the separation is reduced the termination and radiation losses decrease, as does the energy storage. The decrease in radiation losses tends to increase Q as the separation is decreased. It may be concluded that the maximum Q obtainable with the parallel wire line is a bounded quantity and that increasing the termination diameter indefinitely would not improve the Q factor greatly.

The crossing on Figure 7.2 at a length of 2" is due to the energy storage decreasing faster (as s decreases) than the losses. At longer lengths the length factor overcomes this phenomenon.

At lengths greater than those at which the termination losses have become negligible, the Q tends to level off since both energy storage and losses are then proportional to length.

The effect of the contact resistance between conductors and terminations has been neglected.

5. Contrary to former findings, but in collaboration of Pearse's hint, the radiation resistance has been

found to vary with length. There are three factors which might contribute to this variation.

First, the radiation resistance is possibly dependent on the surface condition of the conductors. It seems reasonable that small discontinuities on the surfaces would tend to disperse the waves travelling along the conductors and result in a net outward flow of power. If these discontinuities were uniformly distributed with length, then this would account for the direct variation with length.

Second, the measurements are taken perforce when the section is an even number of half wavelengths long, and each increase in length adds another null in the standing wave pattern. The inclusion of another null in the pattern would increase the field distortion on the line, and hence the radiation.

Third, if the section were not geometrically precise, the variations in the characteristic impedance of the line due to variations in the separation or diameters of the conductors, would cause radiation. The power in the line would be diffused, and hence radiated, upon reflection by terminations which were not exactly parallel or at right angles to the plane containing the conductors. The roughness of the conducting surfaces of the terminations would also contribute to the radiation.

RECOMMENDATIONS.

As I have already stated in the Conclusions,I feel that the Q value of the parallel wire resonant sections is a bounded quantity,and that it might be extended further by a more judicious choice of dimensions;however,the question of the Q's themselves has been thoroughly investigated.

I feel that any further research in this field should be directed towards the inclusion of the resonators in some circuit,so that their usefulness might be more fully demonstrated.

If the measurements are continued I would advise that the magic tee be matched in the conventional manner (post and iris) before it is used. The components required to test such a match are now available in the Department.

Some sketchy results were obtained during the experimentation for conductors of rectangular cross section. These results were low and inconclusive,but the possibility that higher Q values might be obtained with conductors of other than circular cross section has not been fully investigated.

In any further research I think that a different measurement technique might be used. A great deal of automation could be intro duced into the present method in order to reduce the required steps in the procedure. Perhaps the Lecaine

comparison method might be adapted to use with single ended resonators. The combination of basic computer circuitry with microwave techniques, in some device which would yield results automatically, has a great many possibilities.

APPENDIX I

Evaluation of $\int H^2 da$.

Both the expression for the stored energy and the termination losses contain the integral of the magnetic field squared over some area. The expression for the transmitted power also contains this integral. Thus it is imperative that it be evaluated.

The value of the total integral, k, may be derived from the following identity:

$$Q_c = Q_T \frac{L_c}{L_c+L_t+L_r} \qquad 2.26$$

If we substitute for these quantities we obtain

$$k = 4\pi \cosh^{-1} (s/d)$$

It is possible to evaluate k' by numerical integration. The reason for the numerical integration is that the integral cannot be simply evaluated over the circular area of the terminations. The field lines and the circular boundary of the terminations are not compatible in the co-ordinate system used. The possibility of transforming the fields to a system in which the field lines be-

came the axes, viz: biaxial coordinates, was investigated.[10] Although this frame of reference would facilitate any other integration, it is of no use in the present problem. The formidable task of integrating the fields numerically by subdividing the area of the termination, calculating an appropriate value for each area element, and summing the individual areas was performed at least once. It was felt that the effort involved did not warrant a calculation of the losses for all conductor diameters and spacings. Typical values of the magnetic field found during the calculations are shown in Figure I.1.

An effort was made to find a conformal mapping in which the area of integration transformed to an area over which the integral could be easily evaluated. It was in this manner that a more elegant solution of the problem was discovered.

A conformal mapping which transformed the area of the termination exclusive of the area covered by the terminations, into the region between two concentric circles was found in the dictionary compiled by Kober.[11] The area outside of the termination was transformed into a non-concentric circle within the two others.

The procedure involved in theuse of a conformal mapping technique is to: first, express the integrand in terms of the new coordinates; second, transform the area

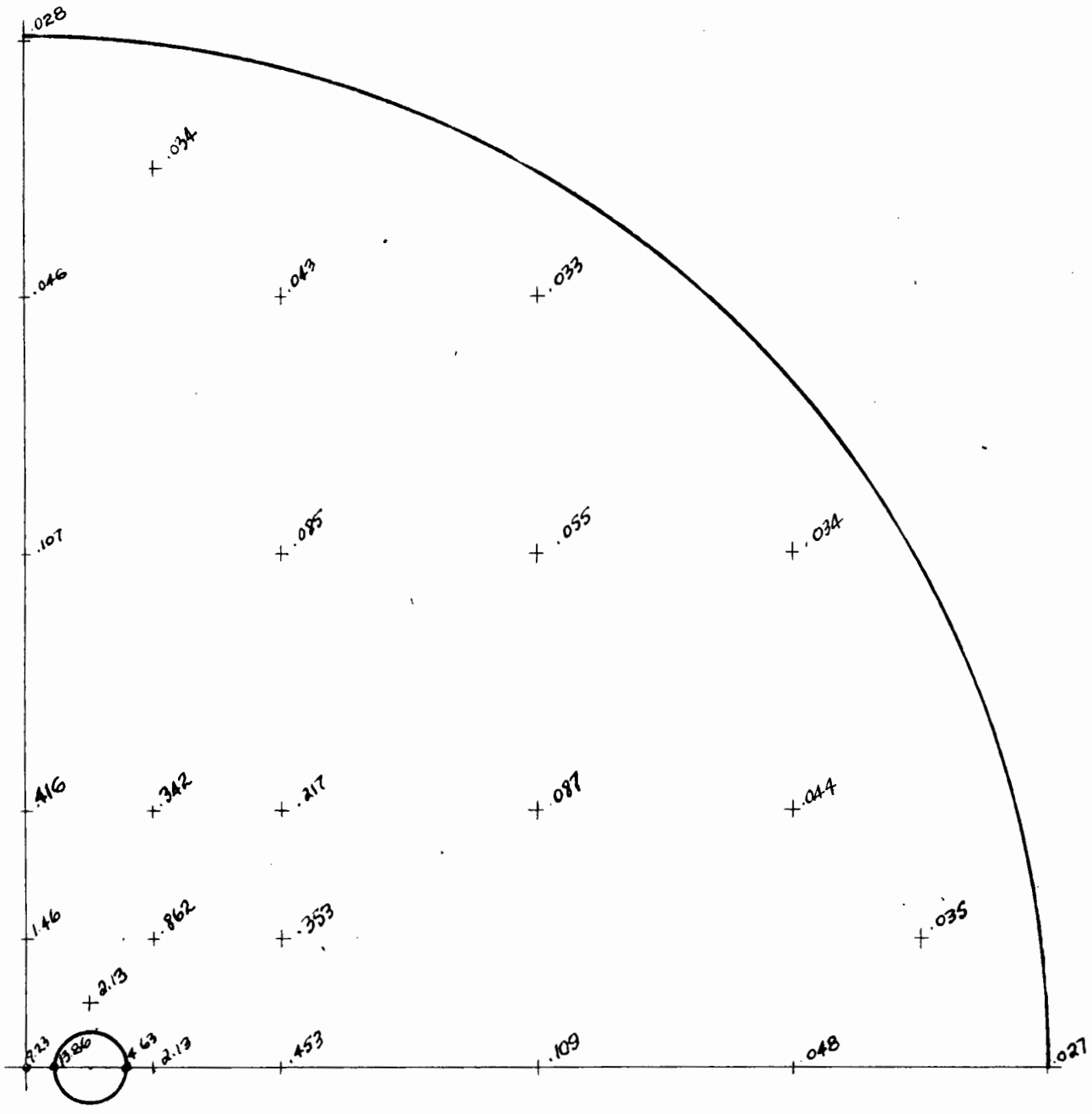

Figure I.1 Values of $(\frac{2\pi}{I})\,|H|$ on a quadrant of termination.

Conductor diameter = 0.25". Separation = 0.50".

element; and third, find the new limits of integration.

As a preliminary step, transpose the axes in the original reference frame so that the center of one conductor lies at the origin, and the line joining the centers lies along the x-axis. In this z-plane:

$$H^2 = (I/2\pi)^2 \frac{4a^2}{\left\{[x-(\frac{1}{2}s+a)]^2+y^2\right\}\left\{[x-(\frac{1}{2}s-a)]^2+y^2\right\}} \qquad 2.28$$

The conformal transformation is then

$$w = \frac{nR_1}{r}\frac{z-m}{z-n} \ , \qquad 2.29$$

where $w = u + iv$,

and m and n are the roots of the following equations.

$$mn = r^2$$
$$(s-m)(s-n) = r^2 \qquad 2.30$$

r is the radius of the conductors.

Now, solving for m and n,

$$m = \tfrac{1}{2}s + a$$
$$n = \tfrac{1}{2}s - a \qquad 2.31$$

and, $s = m + n$

The transformation may be separated into real and imaginary parts to yield u and v in terms of x and y, and vice versa.

$$u = \frac{nR_1}{r} \frac{(x-n)(x-m) + y^2}{(x-n)^2 + y^2}$$

$$v = \frac{nR_1}{r} \frac{y(m-n)}{(x-m)^2 + y^2}$$

$$x = \frac{nC^2v^2 + (1-Cu)(m-mCu)}{C^2v^2 + (1-Cu)^2}$$

$$y = \frac{Cv(m-n)}{C^2v^2 + (1-Cu)^2} \qquad 2.32$$

where

$$C = \frac{r}{nR_1}$$

If we substitute for x and y in Eq. 2.28, we find the form of H^2 in the w-plane.

$$H^2 = (I/2\pi)^2 \frac{C^2v^2 + (1-Cu)^2}{C^2(m-n)^2 \left[u^2 + v^2\right]} \qquad 2.33$$

The area elements in the two planes are related by the formula:[12]

$$du\ dv = J\ dx\ dy \qquad 2.34$$

where J is the Jacobian of the transformation.

$$J = \begin{vmatrix} \frac{\delta u}{\delta x} & \frac{\delta u}{\delta y} \\ \frac{\delta v}{\delta x} & \frac{\delta v}{\delta y} \end{vmatrix}$$

When the partial derivatives are evaluated it is found that

$\frac{\delta u}{\delta x} = \frac{\delta v}{\delta y}$ and that $\frac{\delta u}{\delta y} = -\frac{\delta v}{\delta x}$; as should be so for an analytic function.

and,

$$J = \left(\frac{nR_1}{r}\right)^2 \frac{[C^2v^2 + (1-Cu)^2]^2}{(m-n)^2} \qquad 2.35$$

Therefore, the surface integral of H^2 in the w-plane

$$\int H^2 du\, dv = (I/2\pi)^2 \int \frac{du\, dv}{u^2+v^2} \qquad 2.36$$

Making the substitutions,

$$u = r\cos\theta$$
$$v = r\sin\theta$$
$$du\, dv = r\, dr\, d\theta$$

the integral in polar coordinates in the w-plane is

$$(I/2\pi)^2 \int \frac{dr\, d\theta}{r} \qquad 2.37$$

This is a surprisingly simple integral. It is certainly not obvious or expected. The integral is separable, which is a great simplification in any integration. The remainder of the problem is to determine the limits of integration.

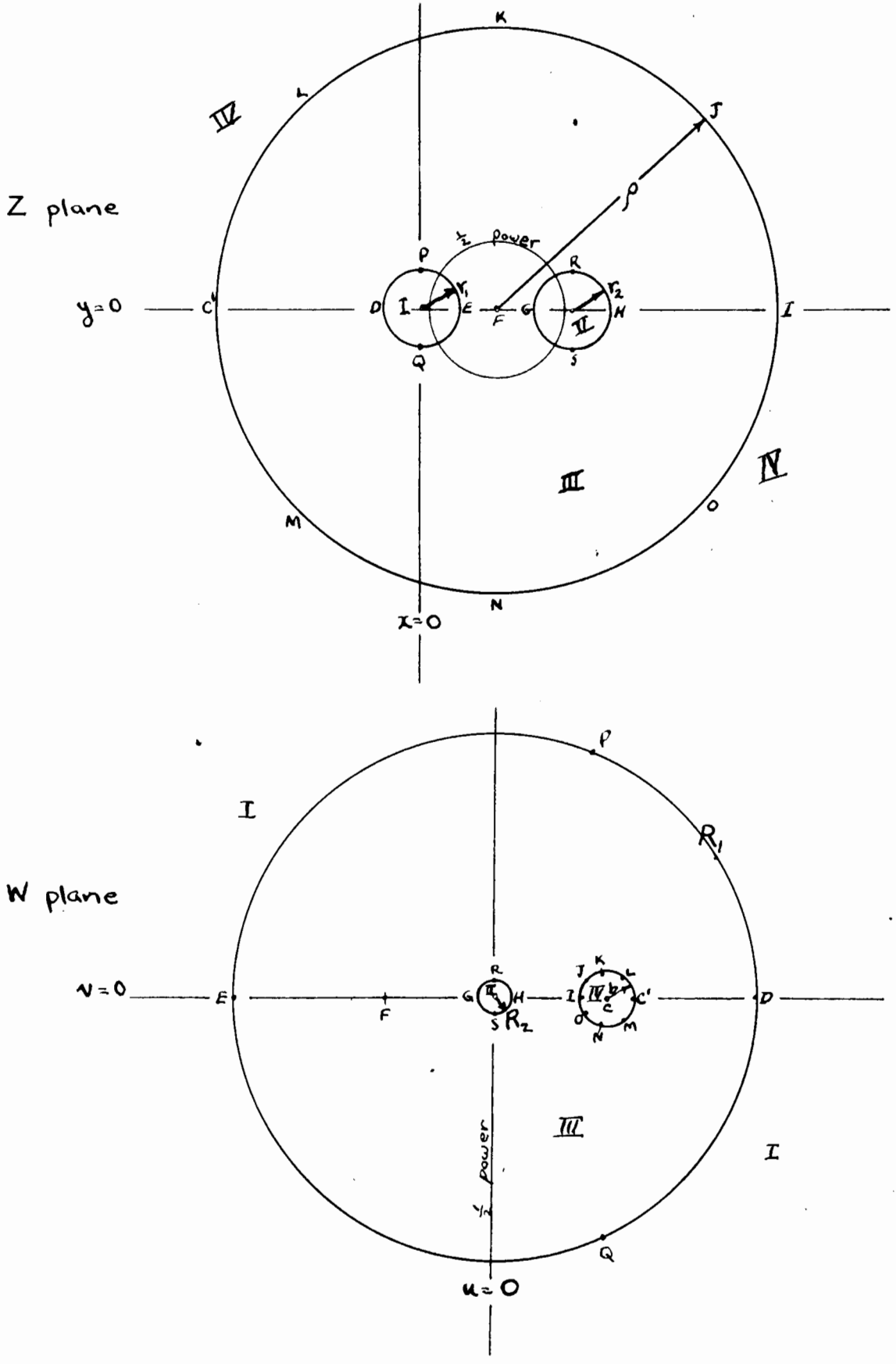

Figure I.2 Illustration of the conformal mapping,

$$w = \frac{nR_1}{\quad} \frac{z-m}{z-n}$$

To determine the limits of integration, it is simplest to find what loci the boundaries in the z-plane become in the w-plane. Figure I.2 shows the transformation graphically. Corresponding points, circles and lines are shown. The explicit mapping expressions for several points are given in Appendix III.

It can be seen that the limits for the evaluation of k are,

$$r = R_2\left(\frac{n}{m}R_1\right) \text{ to } R_1$$

$$\theta = 0 \text{ to } 2\pi \qquad 2.38$$

The limits on the integration over the circle representing the area exterior to the terminations are not as simple because the circle has its center at the point c, rather than the origin. Let the radius of the circle be b. By a suitable transposition,

$$r\cos\psi = u-c$$
$$r\sin\psi = v$$

the integral becomes,

$$I = 2\int_{r=0}^{r=b}\int_{\psi=0}^{\psi=\pi}\frac{r\,dr\;d\psi}{r^2+c^2+2rc\cos\psi} \qquad 2.39$$

and

$$I = 4\pi \cosh^{-1} \frac{c^2-b^2}{c^2}$$

substituting the values of c and b from Appendix III,

$$I = 4\pi \cosh^{-1} \frac{\rho^2}{(\rho^4 - a^4)^{\frac{1}{2}}} \qquad 2.40$$

$$I = 2\pi \ln \frac{\rho^2 + a^2}{\rho^2 - a^2}$$

Integrating equation 2.37 over the limits of 2.38 and thus evaluating k,

$$k = 4\pi \cosh^{-1}(s/d) \qquad 2.41$$

which agrees with the value of k obtained from the identity given earlier.

Thus,

$$k' = 4\pi \left[\cosh^{-1}(s/d) - \cosh^{-1} \rho^2 / \sqrt{\rho^4 - a^4} \right] \qquad 2.42$$

Notice that the circle $\left| z - \frac{(m+n)}{2} \right| = \frac{m-n}{2}$ transforms to the line u=0. In other words the area within the circle becomes one-half of the area of integration, and so one half of the power in the field is transmitted within this circle. This circle has its center midway between the conductors and has a radius = a. It is now evident why Southworth[13] speaks of this circle as the half-power circle. As far as I know he is the only one who has ever

intimated in print that he has successfully integrated the fields of a parallel-wire line without approximations. I believe that the value of k' has been evaluated here for the first time.

Since $\rho \gg a$, in most cases $k \doteq k'$; and most of the field is contained within the terminations. The integrand depends on H^2, however, and since the fields are small away from the conductors the losses would be much smaller. From the numerical integration with $\frac{1}{4}$" conductors $\frac{1}{2}$" apart the terminations contained about 96% of the field.

The termination losses as a function of $(\frac{s}{d})$, with $(\frac{\rho}{d})$ as a parameter, have been plotted in Figure I.3. The upper limit of the graph is the line

$$\frac{Lt}{2\pi R_s} = 2 \cosh^{-1} (\frac{s}{d})$$

and the lower limit has been taken as the locus of the points for which

$$\rho \geq \tfrac{1}{2}(s + d)$$

i.e. the termination covering the complete area of the conductors.

This graph may be used to find k or k' by reading the horizontal axis as $\frac{k}{2\pi}$ or $\frac{k'}{2\pi}$ and finding its value for the proper intersection of $\frac{\rho}{d}$ with $\frac{s}{d}$, or $2\cosh^{-1}(\frac{s}{d})$ with $\frac{s}{d}$, respectively.

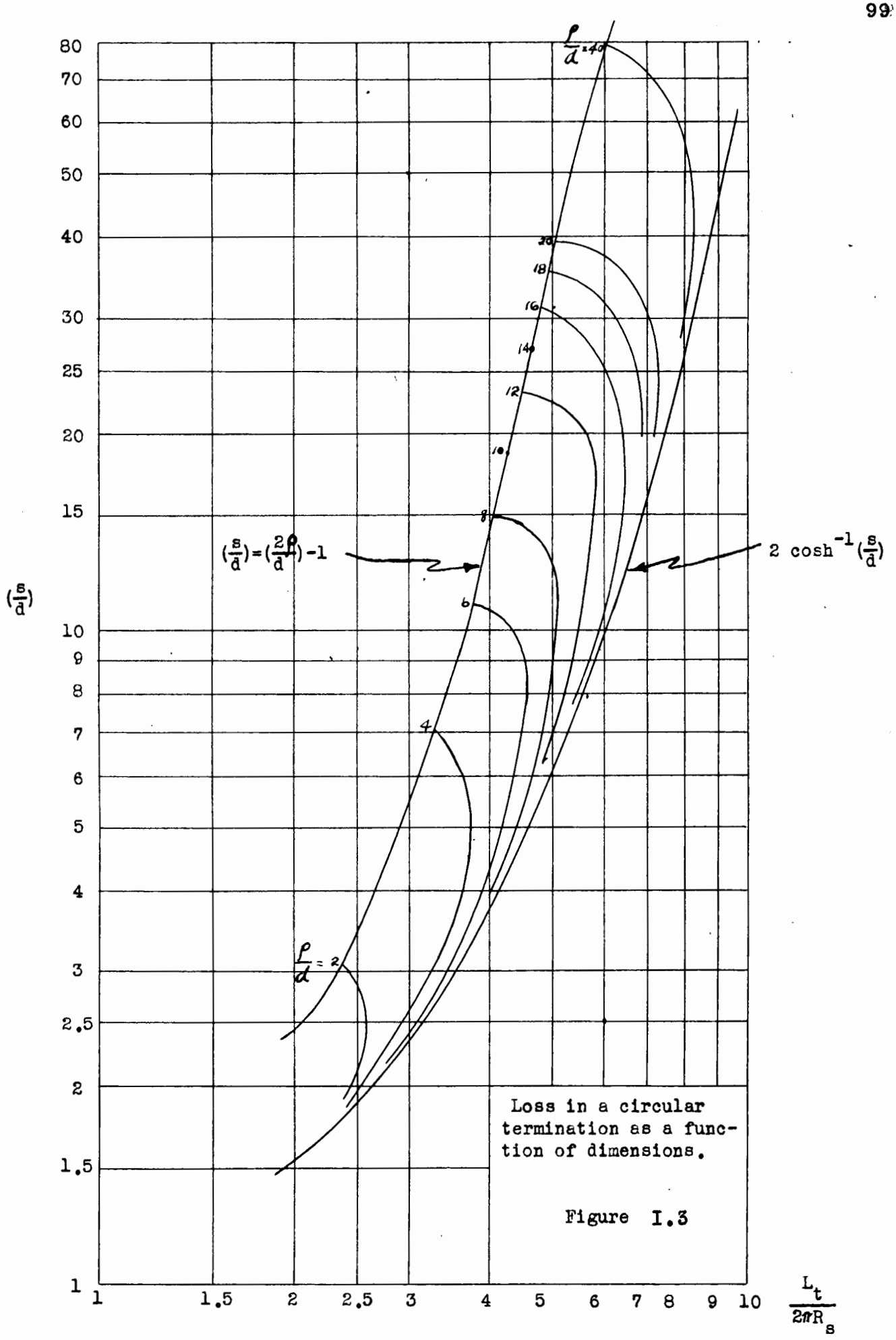

Loss in a circular termination as a function of dimensions.

Figure I.3

APPENDIX II

The variation of the reflection coefficient of a probe coupled resonator with frequency.

A probe coupled resonator may be represented by the following equivalent transformer circuit.

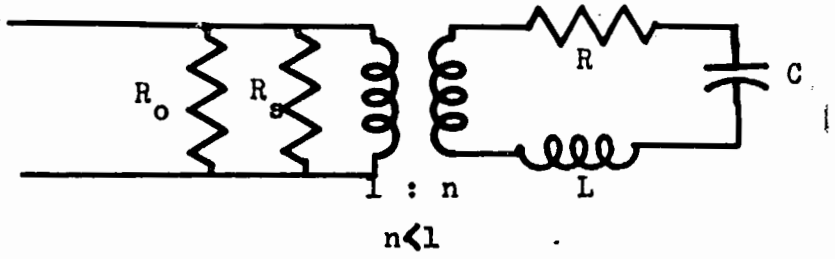

Which, as seen by the resonator, is

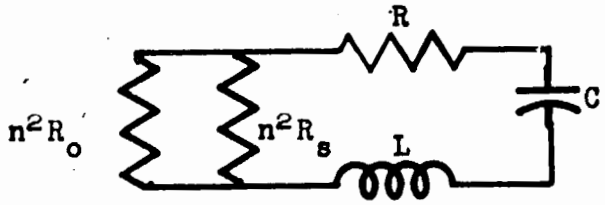

and as seen by the transmission line is

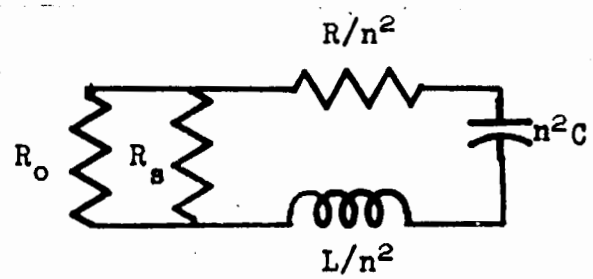

The input impedance of the resonator, as seen by the transmission line, may be expressed as

$$Z_{in} = \frac{1}{\frac{1}{R_s} + \frac{1}{\frac{R}{n^2} + \frac{j}{n^2}(\omega L - \frac{1}{\omega C})}} \qquad \text{II.1}$$

Using the definitions,

$$\omega_o^2 = \frac{1}{LC} \qquad \text{II.2}$$

$$M = \frac{L}{C} \qquad \text{II.3}$$

$$\Delta\omega = \omega - \omega_o \qquad \text{II.4}$$

and assuming that $\omega = \omega_o$, the input impedance, normalized with respect to the characteristic impedance of the transmission line, is:

$$\frac{Z_{in}}{R_o} = \frac{1}{\frac{R_o}{R_s} + \frac{1}{\frac{R}{n^2 R_o} + j\frac{2M}{n^2 R_o}\frac{\Delta\omega}{\omega_o}}} . \qquad \text{II.5}$$

Recalling the definitions of Q, we see from the equivalent circuit diagrams that,

$$Q_o = \frac{\omega_o L}{R} = \frac{M}{R} , \qquad \text{II.6}$$

$$Q_E = \frac{\omega_o L}{n^2 R_o} = \frac{M}{n^2 R_o} \qquad \text{II.7}$$

Equation II.5 may now be expressed as

$$\frac{Z_{in}}{R_o} = \frac{1}{\frac{R_o}{R_s} + \frac{1}{\frac{R}{n^2 R_o} + j\, 2Q_E \frac{\Delta\omega}{\omega_o}}} \qquad \text{II.8}$$

The input impedance off resonance, where the resonator impedance is very high, becomes

$$\frac{Z_{in}}{R_o} = \frac{R_s}{R_o} \qquad \text{II.9}$$

and at resonance, where $\Delta\omega = 0$, becomes:

$$\frac{Z_{in}}{R_o} = \frac{1}{\frac{R_o}{R_s} + \frac{n^2 R_o}{R}} \qquad \text{II.10}$$

From the definition of the reflection coefficient

$$r = \frac{\frac{Z_{in}}{R_o} - 1}{\frac{Z_{in}}{R_o} + 1} \qquad \text{II.11}$$

we find that the reflection coefficient off resonance, r_1, is

$$r_1 = \frac{\frac{R_s}{R_o} - 1}{\frac{R_s}{R_o} + 1} \qquad \text{II.12}$$

Because the coupling losses are small compared to the characteristic impedance of the line, we must take $R_s \gg R_o$. Thus, r_1 is approximately equal to +1 in most cases.

The reflection coefficient at resonance, r_o, is

$$r_o = \frac{\dfrac{1}{\dfrac{R_o}{R_s} + \dfrac{n_2 R_o}{R}} - 1}{\dfrac{1}{\dfrac{R_o}{R_s} + \dfrac{n^2 R_o}{R}} + 1} \quad . \qquad \text{II.13}$$

Rearranging,

$$\frac{R_s}{R_o} = \frac{1 + r_1}{1 - r_1} \quad , \qquad \text{II.14}$$

$$\frac{R_o}{R_s} + \frac{n^2 R_o}{R} = \frac{1 - r_o}{1 + r_o} \quad , \qquad \text{II.15}$$

and

$$\frac{n^2 R_o}{R} = \frac{2(r_1 - r_o)}{(1+r_o)(1+r_1)} \qquad \text{II.16}$$

From equations II.6 and II.7

$$\frac{Q_E}{Q_o} = \frac{R}{n^2 R_o} = \frac{(1+r_o)(1+r_1)}{2(r_1 - r_o)} \qquad \text{II.17}$$

In the critically coupled case $Q_E = Q_o$, and equation II.15 yields $r_o = 0$ since $\frac{R_o}{R_s} \ll 1$.

In the undercoupled case, $Q_E > Q_o$, and r_o is positive.

In the overcoupled case, $Q_E < Q_o$,and r_o is negative.

It may be seen from equation II.17 that a large value of n corresponds to overcoupling,and that a small value to undercoupling. From equation II.10 it may beeseen that,

$$\frac{Z_{in}}{R_o} < 1 \quad \text{for overcoupling,}$$

and that $$\frac{Z_{in}}{R_o} > 1 \quad \text{for undercoupling.}$$

This indicates a shift in the VSWR pattern on the input line of 90 degrees as the cavity goes off resonance if it is overcoupled,and no shift if it is undercoupled,since the detuned resonator is equivalent to an open circuit. ($Z_{in} \to \infty$).

In order to obtain an expression for the reflection coefficient analogous to that for a leep coupled resonator,we define

$$\delta = Q_E \frac{2\Delta\omega}{\omega_o} \quad , \qquad \text{II.18}$$

then equation II.8 becomes

$$\frac{Z_{in}}{R_o} = \frac{1}{\frac{1-r_1}{1+r_1} + \frac{2(r_1-r_o)}{(1+r_o)(1+r_1) + j2\delta(r_o-r_1)}} \qquad \text{II.19}$$

Using equation II.11, we may express the reflection coefficient as

$$r = \frac{r_o(1+r_1)^2 + jr_1 2\delta(r_1-r_o)}{(1+r_1)^2 + j2\delta(r_1-r_o)} \quad , \qquad \text{II.20}$$

and its modulus squared as

$$|r|^2 = \frac{r_o^2(1+r_1)^4 + 4r_1^2(r_1-r_o)^2\delta^2}{(1+r_1)^4 + 4(r_1-r_o)^2\delta^2} \qquad \text{II.21}$$

APPENDIX III

Explicit expressions for the conformal transformation

$$w = \frac{nR_1}{r} \frac{z-m}{z-n}$$

z plane	w plane
Point 0 , 0	Point $-\frac{mR_1}{r}$,0
m+n , 0	$\frac{n^2R_1}{mr}$,0
-r, 0	$+R_1$,0
+r, 0	$-R_1$,0
$\frac{m+n}{2}$, 0	$-\frac{nR_1}{r}$,0
m+n-r, 0	$-\frac{n}{m} R_1$,0
m+n+r, 0	$\frac{n}{m} R_1$,0
0, ir	$R_1 \frac{2\sqrt{mn}}{m+n}$,$R_1 \frac{m-n}{m+n}$
0,-ir	" ,$- R_1\frac{m-n}{1m+n}$
m+n ,$\pm$ir	$\frac{n}{m} R_1 \frac{2\sqrt{mn}}{m+n}$,$\mp\frac{n}{m} R_1 \frac{m-n}{m+n}$
$\frac{m+n}{2}$,$\pm$ iρ	$\frac{nR_1}{r} \frac{4\rho^2-(m-n)^2}{4\rho^2+(m-n)^2}$,$\frac{nR_1}{r} \frac{4\rho(m-n)}{4\rho^2+(m-n)^2}$

z plane	w plane
$\frac{m+n}{2} + \frac{\rho}{\sqrt{2}}, \pm \frac{\rho}{\sqrt{2}}$	$\frac{nR_1}{r} \frac{4\rho^2-(m-n)^2}{4\rho^2+(m-n)^2+2\sqrt{2}\rho(m-n)}$, $\pm \frac{2\sqrt{2}\rho(m-n)}{4\rho^2+(m-n)^2+2\sqrt{2}\rho(m-n)}$
$\frac{m+n}{2} - \frac{\rho}{\sqrt{2}}, \pm \frac{\rho}{\sqrt{2}}$	$\frac{nR_1}{r} \frac{4\rho^2-(m-n)^2}{4\rho^2+(m-n)^2-2\sqrt{2}\rho(m-n)}$, $\pm \frac{2\sqrt{2}\rho(m-n)}{4\rho^2+(m-n)^2-2\sqrt{2}\rho(m-n)}$
$\frac{m+n}{2} - \rho$, 0	$\frac{2+(m-n)}{2-(m-n)}$, 0
$\frac{m+n}{2} + \rho$, 0	$\frac{2-(m-n)}{2+(m-n)}$, 0
Circle $\lvert z \rvert = r$	Circle $\lvert w \rvert = R_1$
$\lvert z - (m+n) \rvert = r$	$\lvert w \rvert = \frac{n}{m} R_1 = R_2$
$\lvert z - \frac{(m+n)}{2} \rvert = \rho$	$^{*}\left\lvert w - \frac{nR_1}{r} \frac{4\rho^2+(n-m)^2}{4\rho^2-(n-m)^2} \right\rvert$ $= \frac{nR_1}{r} \frac{4\rho(m-n)}{4\rho^2-(n-m)^2}$

* See footnote on next page.

z plane	w plane
Line $x = m+n$	Circle $\left\|w - \frac{nR_1}{r}\frac{m+n}{2m}\right\| = \frac{nR_1}{r}\frac{m-n}{2m}$
$x = 0$	$\left\|w - \frac{R_1}{r}\frac{m+n}{2}\right\| = \frac{R_1}{r}\frac{m-n}{2}$
power circle, $\left\|z - \frac{m+n}{2}\right\| = \frac{m-n}{2}$	Line, $u = 0$
Minimum value of ρ, $\left\|z - \frac{m+n}{2}\right\| = \frac{m+n}{2} + r$	$\left\|w - \frac{R_1}{2}(1+\frac{n}{m})\right\| = \frac{R_1}{2}(1-\frac{n}{m})$

Footnote.

The values of c and b as shown on Figure I.2 are

$$c = \frac{nR_1}{r}\,\frac{4\rho^2 + (n-m)^2}{4\rho^2 - (n-m)^2}$$

$$b = \frac{nR_1}{r}\,\frac{4\rho(m-n)}{4\rho^2 - (n-m)^2}$$

APPENDIX IV

The purpose of this appendix is to demonstrate qualitatively that the matched condition of a magic tee may be indicated by the use of a movable short circuit termination.

A magic tee, when terminated by matched generator and detector, has this property: if power is delivered to the H arm of the tee, and one side arm is terminated in a matched load, then the voltage in the E arm is directly porportional to the reflection coefficient of the termination on the other side arm.

The reflection coefficient, k_{11}, of the termination, Z_{T1}, on this side arm is defined as

$$k_{11} = \frac{Z_{T1} - Z_0}{Z_{T1} + Z_0} \quad ,$$

where Z_0 is the characteristic impedance of the transmission line forming the side arm of the tee.

If Z_{T1} is a movable short circuit, then $Z_{T1} = -jZ_0 \tan\beta x$. βx is the electrical distance from the short to the reference plane at which Z_{T1} is measured.

Therefore:

$$k_{11} = \frac{-jZ_0 \tan\beta x - Z_0}{-jZ_0 \tan\beta x + Z_0}$$

or $$k_{11} = \frac{(1 - \tan^2\beta x) + j2\tan\beta x}{1 + \tan^2\beta x}$$

The power flowing in the E arm is porportional to $|k_{11}|^2$, which is the quantity measured by a square-law detector, so

$$|k_{11}|^2 = \frac{(1-\tan^2\beta x)^2 + 4\tan^2\beta x}{(1+\tan^2\beta x)^2}$$

i.e., $$|k_{11}|^2 \equiv 1$$

Since this is an identity independent of the value of βx, and hence the position of the short, it may be seen that the output of a matched magic tee is independent of the position of a movable short connected to one side arm, providing the other side arm is matched.

BIBLIOGRAPHY

Reference

1 Montgomery,C.G.,"Technique of Microwave Measurements",M.I.T. Radiation Laboratory Series,vol. 11. McGraw-Hill Book Company,Inc. New York 1947.

2 Hoy,N.A.,"The Effects of Radiation on the Properties of Half-Wavelength Resonant Unshielded Parallel Wire Transmission Lines,in the Frequency Range 300-1300 Mc/s." M.Eng. Thesis. McGill University,April 1950.

Carr,E.F.,"The Effects of Radiation on the Properties of Quarter Wavelength Resonant Unshielded Parallel-Wire Transmission Lines,in the Frequency Range 300 mc/s to 1300 mc/s." M.Eng. Thesis. McGill University. April 1950.

Boucher,J.E.,"Resonance Characteristics of Transmission Line Circuits". M.Eng. Thesis. McGill University. August 1951.

Yurko,M.,"The Radiation Resistance of Resonant Transmission Lines". M.Eng. Thesis. McGill University. August 1951.

Chipman,R.A., et al,"The Radiation Resistance of Resonant Transmission Lines". Journal of Applied Physics,vol 23,no 6,pp 613-620. June 1952.

Chipman,R.A.,"Effect of Radiation on Resonant Lines"? Electronics. June 1953.

3 Pearse,C.D.,"High-Q Resonant Circuits in the Frequency Range 600 Mc/s to 1600 Mc/s using Parallel-Wire Transmission Lines". M.Sc.Thesis. McGill University. August 1954.

4 Chipman,R.A.,"A Resonance Curve Method for the Absolute Measurement of Impadance at Frequencies of the Order 300 Mc/Second". Journal of Applied Physics, vol 10,no 1, January 1939.

5 King,D.D.,"Measurements at Centimeter Wavelengths". D.Van Nostrand Company,Inc. New York 1952.

6 Hamilton,D.R.,J.K.Knipp,and J.B.H. Kuper,"Klystron and Microwave Triodes". M.I.T. Radiation Laboratory Series,vol 7,sec 15-3. McGraw-Hill Book Company,Inc. New York 1948.

7 Sproull,R.L.,and E.G.Linder,"Resonant Cavity Measurements",Proc.I.R.E.,vol 34, pp 305-312. May 1946.

8 Lecaine,H.,"The Q of a Microwave Cavity by Comparison with a Calibrated High-Frequency Circuit", Proc.I.R.E.,vol 40, pp 1556157. February 1952.

9 Reed,E.D.,"Measurement of Q by Reflected Power", Proceedings of the National Electronics Conference, vol 7,pp 162-172. 1951. Also Bell System Technical Publications,Monograph number 1953.

10 Stratton,J.A.,"Electromagnetic Theory",McGraw-Hill Book Company,Inc. New York 1948.

Schelkunoff,S.A.,"Electromagnetic Waves",D.Van Nostrand Company,Inc. New York 1943.

Schelkunoff,S.A.,"Applied Mathematics for Engineers and Scientists", D.Van Nostrand Company,Inc. New York 1948.

11 Kober,H.,"Dictionary of Conformal Representations", Dover Publications,Inc. USA 1952.

12 Franklin,P,"Methods of Advanced Calculus",McGraw-Hill Book Company,Inc. New York 1944.

Southworth,G.C.,"Principles and Applications of Waveguide Transmission",BSTJ, vol XXIX, no 3,p 295. July 1950.

GENERAL REFERENCES consulted by the author but to which no specific reference has been made.

Microwave Theory and Techniques.

Ramo,S., and J.R.Whinnery,"Fields and Waves in Modern Radio",second edition. John Wiley and Sons, Inc. New York 1953.

Reich,H.J.,et al,"Microwave Theory and Techniques", D.Van Nostrand Company,Inc. New York 1953.

Barlow,H.M.,and A.L.Cullen,"Microwave Measurements", Constable and Company Ltd. London 1950.

Saxon,G.,and C.W.Miller,"Magic-Tee Waveguide Junction",Wireless Engineer, vol 25, pg 138. May 1948.

Reflex Klystrons.

"Klystron Technical Manual". Sperry Gyroscope Company, Inc. Great Neck , New York. 1944.

Bleaney,B.,"Electronic Tuning of Reflection Klystrons", Wireless Engineer,Vol XXV,pp 6-11. 1948.

Reed,E.D.," A Coupled Resonator Reflex Klystron", BSTJ, vol XXXII, pp 715-766. May 1953.

Mathematical References.

" Reference Data for Radio Engineers". Third edition. Federal Telephone and Radio Company. 1949.

Dwight,H.B.,"Tables of Integrals and Other Mathematical Data". The MacMillan Company. New York 1947.